The Journal of Immunology

Lineage-Specific Effector Signatures of Invariant NKT Cells Are Shared amongst γδ T, Innate Lymphoid, and Th Cells

You Jeong Lee, Gabriel J. Starrett, Seungeun Thera Lee, Rendong Yang, Christine M. Henzler, Stephen C. Jameson and Kristin A. Hogquist

J Immunol published online 6 July 2016
http://www.jimmunol.org/content/early/2016/07/05/jimmunol.1600643

The Journal of Immunology is published twice each month by The American Association of Immunologists, Inc., 9650 Rockville Pike, Bethesda, MD 20814-3994.

Print ISSN: 0022-1767 Online ISSN: 1550-6606.

Published July 6, 2016, doi:10.4049/jimmunol.1600643

Lineage-Specific Effector Signatures of Invariant NKT Cells Are Shared amongst γδ T, Innate Lymphoid, and Th Cells

You Jeong Lee,* Gabriel J. Starrett,† Seungeun Thera Lee,* Rendong Yang,‡ Christine M. Henzler,‡ Stephen C. Jameson,* and Kristin A. Hogquist*

Invariant NKT cells differentiate into three predominant effector lineages in the steady state. To understand these lineages, we sorted undifferentiated invariant NK T progenitor cells and each effector population and analyzed their transcriptional profiles by RNAseq. Bioinformatic comparisons were made to effector subsets among other lymphocytes, specifically Th cells, innate lymphoid cells (ILC), and γδ T cells. Myc-associated signature genes were enriched in NKT progenitors, like in other hematopoietic progenitors. Only NKT1 cells, but not NKT2 and NKT17 cells, had transcriptome similarity to NK cells and were also similar to other IFN-γ–producing lineages such as Th1, ILC1, and intraepithelial γδ T cells. NKT2 and NKT17 cells were similar to their analogous subsets of γδ T cells and ILCs, but surprisingly, not to Th2 and Th17 cells. We identified a set of genes common to each effector lineage regardless of Ag receptor specificity, suggesting the use of conserved regulatory cores for effector function. ***The Journal of Immunology*****, 2016, 197: 000–000.**

Invariant NKT (iNKT) cells are canonical T cells recognizing lipid Ags in the context of CD1d molecules (1). They are positively selected in the thymic cortex at the $CD24^{hi}$ stage 0 (2) and differentiate into mature $CD24^{low}$ effector subsets that produce IFN-γ, IL-4, or IL-17 in the thymic medulla (3, 4). These subsets were designated as NKT1, NKT2, and NKT17 cells, respectively, and their lineage properties are determined by key transcriptional factors including PLZF, TBET, GATA3, and retinoic acid–related orphan receptor γt (RORγt) (3, 4). Our previous data suggest that a $CD24^{lo}$, but uncommitted, NKT progenitor (NKTp) can give rise to each differentiated subset, and such progenitors were defined as cells negative for IL-17RB and human CD2 (huCD2) among total $PLZF^{hi}$ NKT2 cells in KN2 IL-4 reporter mice (3, 5). In adoptive transfer assays, a fraction of IL-$17RB^{-}huCD2^{-}$ NKT2 cells differentiated into NKT1 cells, whereas IL-$17RB^{+}huCD2^{+}$ NKT2 cells did not. In localization analysis, IL-4–producing $huCD2^{+}$ NKT2 cells were mostly in the thymic medulla, whereas $huCD2^{-}$ NKTp cells were relatively enriched in the cortex, consistent with their developing ontogeny (6). These results indicated there are four different iNKT subsets including a progenitor and three differentiated subsets.

It is increasingly appreciated that these iNKT subsets are analogous to conventional Th cell subsets (4). Not only iNKT cells, but also innate lymphoid cells (ILCs) and γδ T cells, have subsets with distinct effector programs similar to Th cells (7–9). A previous report concluded that iNKT cells share an extensive transcriptional program with NK cells and that this program also operates constitutively in intraepithelial γδ T cells, activated CD8 T cells, and developing thymocytes (8). However, these analyses were based on an outdated staging model of iNKT cell development and thereby analyzed cells that predominantly contained NKT1 cells because of the background mouse strain used. Furthermore, it has not been addressed how the transcriptional nature of innate lymphoid and innate-like T cells and conventional Th cells are correlated with each other.

To address these issues, we performed RNAseq analysis of iNKT subsets, including NKTp, NKT1, NKT2, and NKT17 cells. Importantly, we found only NKT1 cells, but not NKT2 and NKT17 cells, shared a transcriptional program with NK (8), activated CD8 T, and intraepithelial γδ T cells. We also identified that NKTp signature genes were shared among differentiating or proliferating hematopoietic cells including developing thymocytes, which were associated with an upstream regulator Myc protein. Using previously published data sets, we measured the transcriptional similarity of iNKT subsets to those of analogous γδ T cells, ILC, and Th cells (7, 9, 10). Signature genes of NKT1 cells were defined and found to be highly shared with ILC1 and Th1 cells, indicating profound similarity between the transcriptional programs of all IFN-γ–producing cells. NKT2 cells were most similar to thymic $CD24^{low}V\delta6^{+}$ γδ T cells, both of which expressed high levels of PLZF, followed by ILC2. NKT17 cells were similar to thymic $CD24^{low}V\gamma2^{+}$ γδ T cells and ILC3 cells. Although Th2 and Th17 cells shared a small core of effector signature genes with the analogous subsets of ILC, γδ T, and iNKT cells, their overall transcriptional profiles were more distinct. These findings indicate that the transcriptional nature of ILC or innate-like T cells is distinguished from conventional Th cells.

Materials and Methods

Mice

C57BL/6NCr and BALB/c mice were purchased from the National Cancer Institute and The Jackson Laboratory, respectively. BALB/c *Tbx21*^{gfp} $KN2^{+/-}$ were described previously (3). All of the mouse experiments were

*Department of Laboratory Medicine and Pathology, Center for Immunology, University of Minnesota, Minneapolis, MN 55455; †Department of Biochemistry, Molecular Biology and Biophysics, University of Minnesota, Minneapolis, MN 55455; and ‡Supercomputing Institute for Advanced Computational Research, University of Minnesota, Minneapolis, MN 55455

ORCIDs: 0000-0001-5871-5306 (G.J.S.); 0000-0003-4566-2211 (C.M.H.).

Received for publication April 12, 2016. Accepted for publication June 14, 2016.

This work was supported by National Institutes of Health Grants R37-AI39560 (to K.A.H.), RO1-AI075168 (to S.C.J.), and K99-AI114884 (to Y.J.L).

The raw data presented in this article have been submitted to the National Center for Biotechnology Information database under accession number PRJNA318017.

Address correspondence and reprint requests to Dr. You Jeong Lee and Dr. Kristin A. Hogquist, Department of Laboratory Medicine and Pathology, Center for Immunology, University of Minnesota, 2101 6th Street SE, Minneapolis, MN 55455. E-mail addresses: leey@umn.edu (Y.J.L.) and hogqu001@umn.edu (K.A.H.)

The online version of this article contains supplemental material.

Abbreviations used in this article: ETP, early thymic precursor; FDR, false discovery rate; huCD2, human CD2; ILC, innate lymphoid cell; iNKT, invariant NKT cell; IPA, Ingenuity Pathway Analysis; MAIT, mucosal-associated invariant T; NES, normalized enrichment score; NKTp, NKT progenitor; RORγt, retinoic acid–related orphan receptor γt.

performed under protocols approved by the Institutional Animal Care and Use Committee of the University of Minnesota.

Flow cytometry

Biotinylated PBS-57 loaded or unloaded CD1d monomers were obtained from the tetramer facility of the National Institutes of Health. For intracellular staining, single-cell suspensions were surface stained, fixed, and permeabilized with the eBioscience Foxp3 staining buffer set. All Abs were from eBioscience, BD Biosciences, or BioLegend, unless indicated. Cells were analyzed on an LSR II (BD Biosciences), and data were processed with FlowJo software (Tree Star).

Cell isolation and RNA preparation

Thymocytes were isolated from two to three mice per sample from BALB/c *Tbx21*^{gfp} KN2$^{+/-}$ mice, and iNKT cells were enriched by CD1d tetramer pulldown. Briefly, cells stained with PE-conjugated CD1d tetramer were enriched using anti-PE microbeads (Miltenyi Biotec) according to the manufacturer's instruction. TCRβ^{+}CD1d tetramer^{+}CD8^{-}CD24^{-} thymic iNKT cells were separated into four subsets and sorted with an FACSAria (BD Biosciences). An RNeasy mini kit (Qiagen, Redwood City, CA) was used to isolate RNA obtained from each sample.

RNA sequencing

RNA sequencing was done at the University of Minnesota Genomics Center. Total RNA was quantified using a fluorimetric RiboGreen assay, and RNA quality was assessed using capillary electrophoresis and the Agilent RNA Integrity Number (Agilent Technologies). All samples that were submitted for library creation had an RNA Integrity Number of eight or greater. Library creation was performed using Illumina's Truseq RNA Sample Preparation Kit (catalog number RS-122-2001; Illumina). Final library size distribution was validated using capillary electrophoresis and quantified using fluorimetry (PicoGreen) and via quantitative PCR. Indexed libraries are then normalized, pooled, and size selected to 320 bp ± 5% using Caliper's XT instrument (Caliper Life Sciences). Truseq libraries were hybridized to a paired end flow cell, amplified on the Illumina cBot, and subsequently run on the HiSEquation 2000 (Illumina). Raw data are available at the National Center for Biotechnology Information under accession number PRJNA318017.

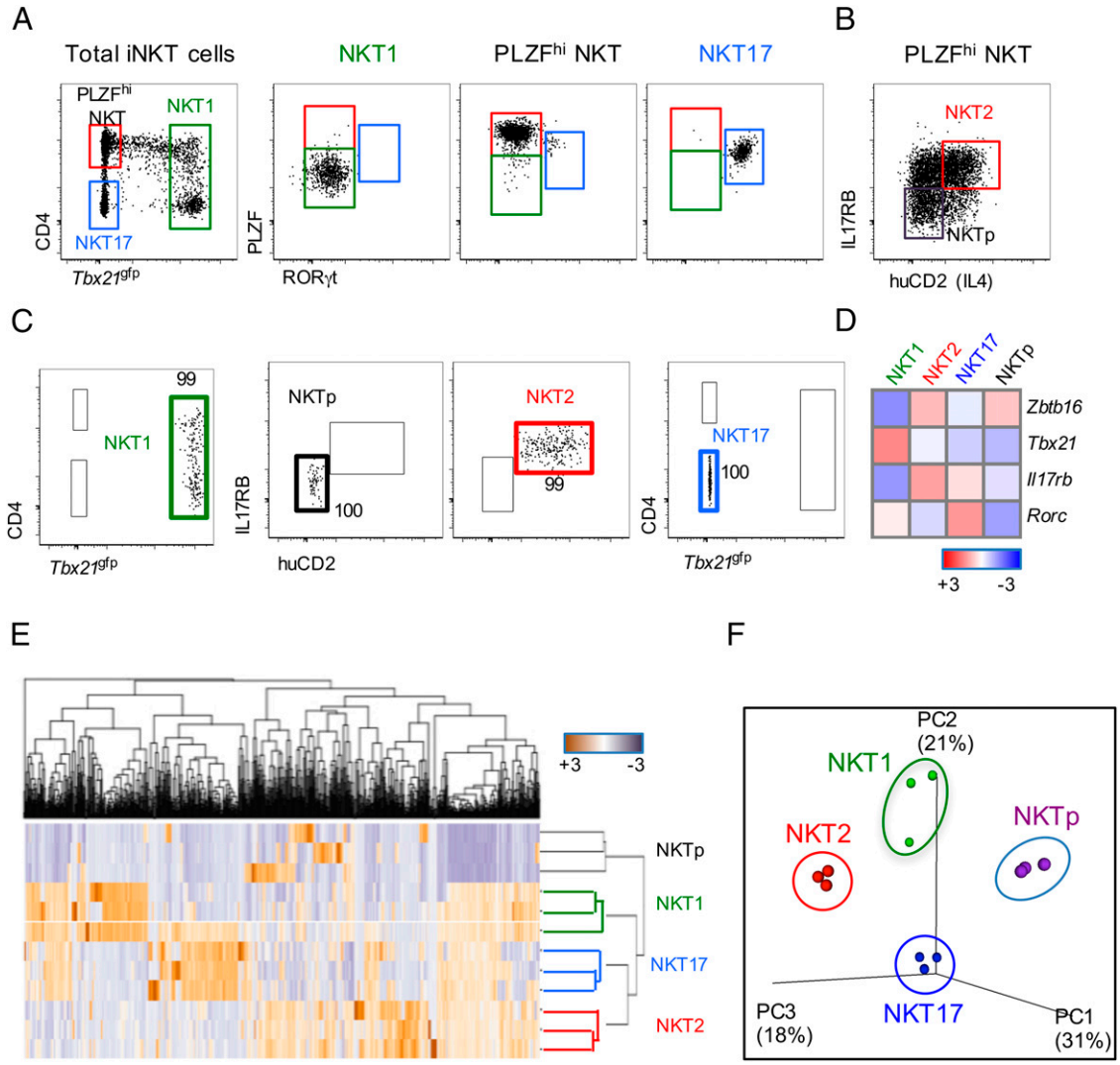

FIGURE 1. iNKT subsets have unique transcriptional profiles. (**A**) Sorting strategy of iNKT subsets using surface markers. Total thymocytes from BALB/c *Tbx21*^{gfp} KN2$^{+/-}$ mice were stained with CD1d tetramer and indicated surface markers and analyzed by their transcription factor profiles. Each subset was designated as NKT1, PLZF^{hi} NKT, and NKT17 cells. (**B**) PLZF^{hi} NKT cells were further separated by expression levels of IL-17RB and human CD2 (huCD2) and designated as NKTp and NKT2 cells. (**C**) Postsort purities of each subset are shown. (**D**) Four different subsets of thymic iNKT cells were sorted as triplicates from cells pooled from two to three mice each and analyzed for their RNA transcripts. Heat map was generated using mean fragments per kb of transcript per million values of triplicates to show their differential expression patterns of PLZF (encoded by *Zbtb16*), TBET (encoded by *Tbx21*), IL-17RB (encoded by *Il17rb*), and RORγt (encoded by *Rorc*). (**E**) Hierarchical clustering of iNKT subsets is shown using the 1000 genes that are most differentially expressed. (**F**) Principal component analysis of gene expression is shown for each iNKT subset. Numbers along axes indicate relative scaling of the principal variables.

Data analysis

We obtained an average of 20 million reads per replicate for triplicates of four different cell types with technical duplicates (total 24 reads). RNAseq reads were aligned to the mouse reference genome (mm10) and most recent transcript annotations using TopHat (v2.0.13) (11). Expression levels of all transcripts were quantified using Cuffquant (12), and differentially expressed genes were determined by Cuffdiff (12). Hierarchical clustering and principal component analysis were performed based on the raw read counts from the top 1000 genes ranked by the variance of their expression values across samples. Volcano plots were generated using Multiplot Studio (Gene Pattern), and heat maps were generated with Gene-E (Broad Institute). For heat map generation, if not otherwise indicated, data were log2-transformed and visualized by relative expression per row with the row mean subtracted and divided by row SD. Rows were grouped by the Pearson correlation coefficient via hierarchical clustering. Gene set enrichment analysis was performed to calculate normalized enrichment score (NES) (13). Prism (GraphPad Software) was used for data plotting, and Venny (http://bioinfogp.cnb.csic.es/tools/venny) was used to visualize Venn diagrams. Cytoscape was used to generate network analysis (14). Upstream regulators and canonical pathway analysis were identified using Qiagen's Ingenuity Pathway Analysis (IPA; Qiagen). We used RNAseq of Th cells from Array Express with the access code E-MTAB-2582 and microarray data from Gene Expression Omnibus with access code GSE37448 for ILC and other cell types including γδ T cells with access code GSE15907.

Results

iNKT subsets have unique genetic profiles with characteristic transcripts

We sorted thymic iNKT subsets from BALB/c Tbet/IL-4 reporter mice (*Tbx21*^{gfp} KN2$^{+/-}$) mice, in which NKT1 cells are CD4$^{+/-}$GFP^{+}, NKT17 cells are CD4^{-}GFP^{-}CD44^{hi}, and PLZF^{hi} NKT2/p cells are CD4^{+}GFP^{-}, among total CD1d tetramer-positive cells (Fig. 1A, left panel). These marker combinations had ~97% overlap with subsets directly defined by transcription factor staining (Fig. 1A, right three panels). PLZF^{hi} NKT cells were further divided into NKT2 and NKTp cells (Fig. 1B), as we previously showed that IL-17RB and huCD2-expressing cells represent terminally differentiated IL-4–secreting NKT2 cells, and IL-17RB and huCD2-negative cells contained progenitors that can give rise to differentiated subsets (3). For efficient cell sorting, we performed CD1d tetramer enrichment and sorted populations that had >99% purity (Fig. 1C). We isolated

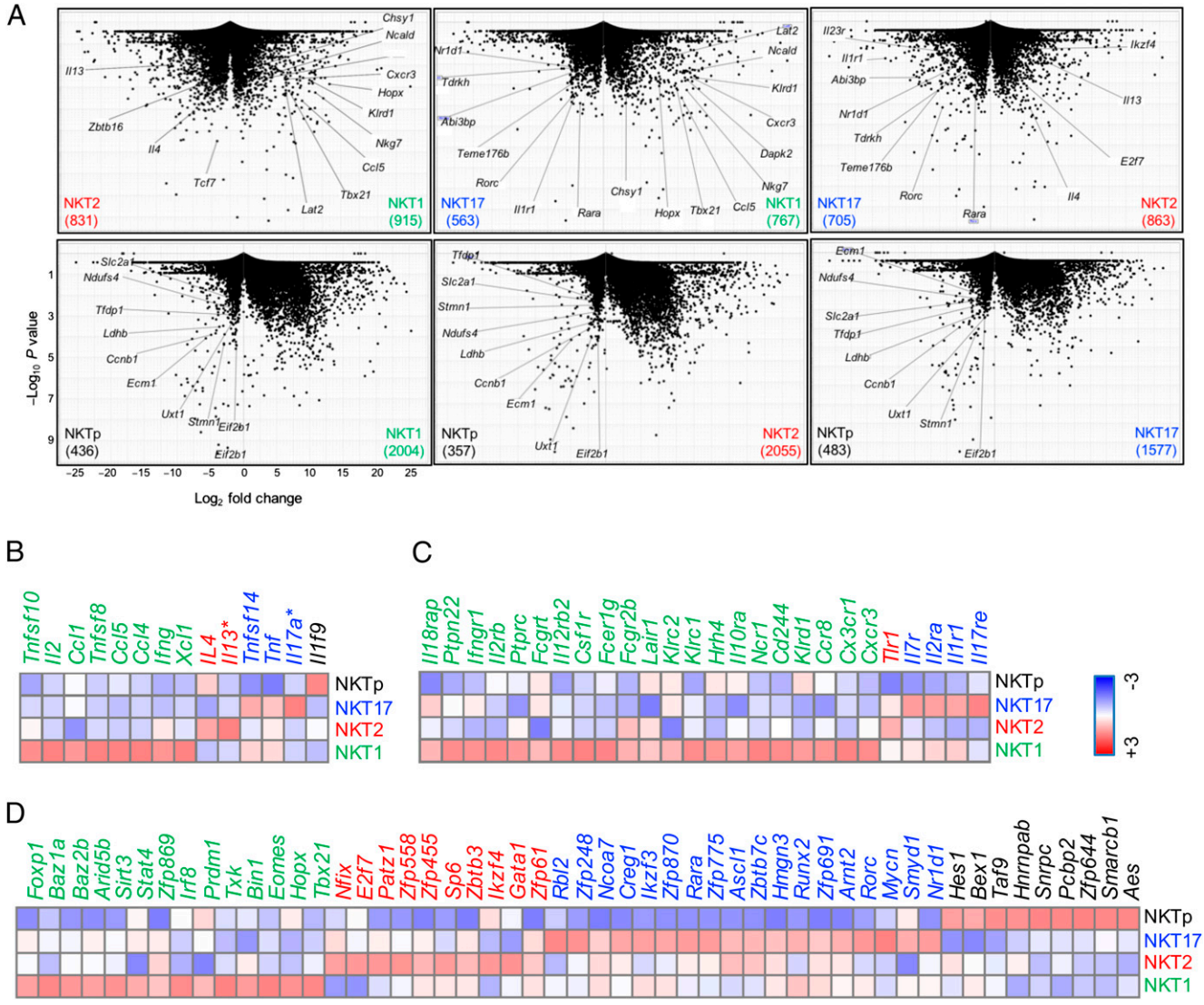

FIGURE 2. Characteristic transcripts of each iNKT subset. (**A**) Volcano plots were generated after pairwise comparisons between two subsets, and numbers in parentheses indicate numbers of genes upregulated at least 2-fold in each subset with p values <0.05. Each symbol represents a single gene. Heat maps show cytokines (**B**), receptors (**C**), and transcription factors (**D**) uniquely expressed in one subset at least 2-fold higher than the other three subsets with significant p values (<0.05). Color coding indicates genes highly expressed in NKT1 (green), NKT2 (red), NKT17 (blue), and NKTp (black) cells. *These two genes had insignificant p values (>0.05) in at least one of three comparisons.

four different subsets in triplicate, prepared RNA, and performed RNAseq analysis. A heat map generated after RNAseq analysis showed each subset was positive for the expected transcription factors (Fig. 1D). Hierarchical clustering analysis, using the 1000 most variable genes among the four subsets, showed that NKTp cells are indeed a unique population that had the least similarity with the other three subsets (Fig. 1E). Principal component analysis confirmed these subsets have distinct transcriptional profiles (Fig. 1F).

Next, we analyzed genes differentially expressed between subsets of iNKT cells. Pairwise comparison of NKT1, NKT2, and NKT17 cells generated three volcano plots showing 563–915 genes at least 2-fold upregulated in each subset with p values <0.05 (Fig. 2A, top panels). NKTp cells showed 3.2- to 5.6-fold fewer significantly upregulated genes compared with the three differentiated subsets, indicating they are transcriptionally less active (Fig. 2A, bottom panels). Using these data, we generated heat maps showing a selected list of genes that are uniquely upregulated in one subset compared with the other three subsets in three different categories, including cytokines (Fig. 2B), receptors (Fig. 2C), and transcription factors (Fig. 2D). *Tbx21* and *Ifng* were highly upregulated in NKT1 cells, and *Il4* and *Rorc* were specific to NKT2 and NKT17 cells, respectively. *Il13* and *Il17a* transcripts were highest in NKT2 and NKT17 cells, respectively, although p values were >0.05 in at least one comparison. GATA3 was not detected as a unique gene of NKT2 cells, as NKT17 cells also expressed it at a similar level (3). NKTp cells had few signature cytokine or receptor transcripts but uniquely upregulated several transcription factors, including transcriptional regulators (*Hes1*, *Taf9*, *Smarcb1*, *Zfp644*, and *Aes*) and ribonuclear proteins (*Hnrnpab* and *Snrpc*), suggesting they have distinctive nuclear protein activity (Fig. 2D).

iNKT subsets have unique signature genes

To further elucidate the transcriptional nature of each iNKT subset, we generated a list of signature genes that were uniquely expressed in each subset, with q values <0.05 compared with the other three subsets as depicted in Fig. 3A and shown in Supplemental Table I. We first looked at how these genes were expressed at different stages of thymic NKT cells, as defined by data from the ImmGen

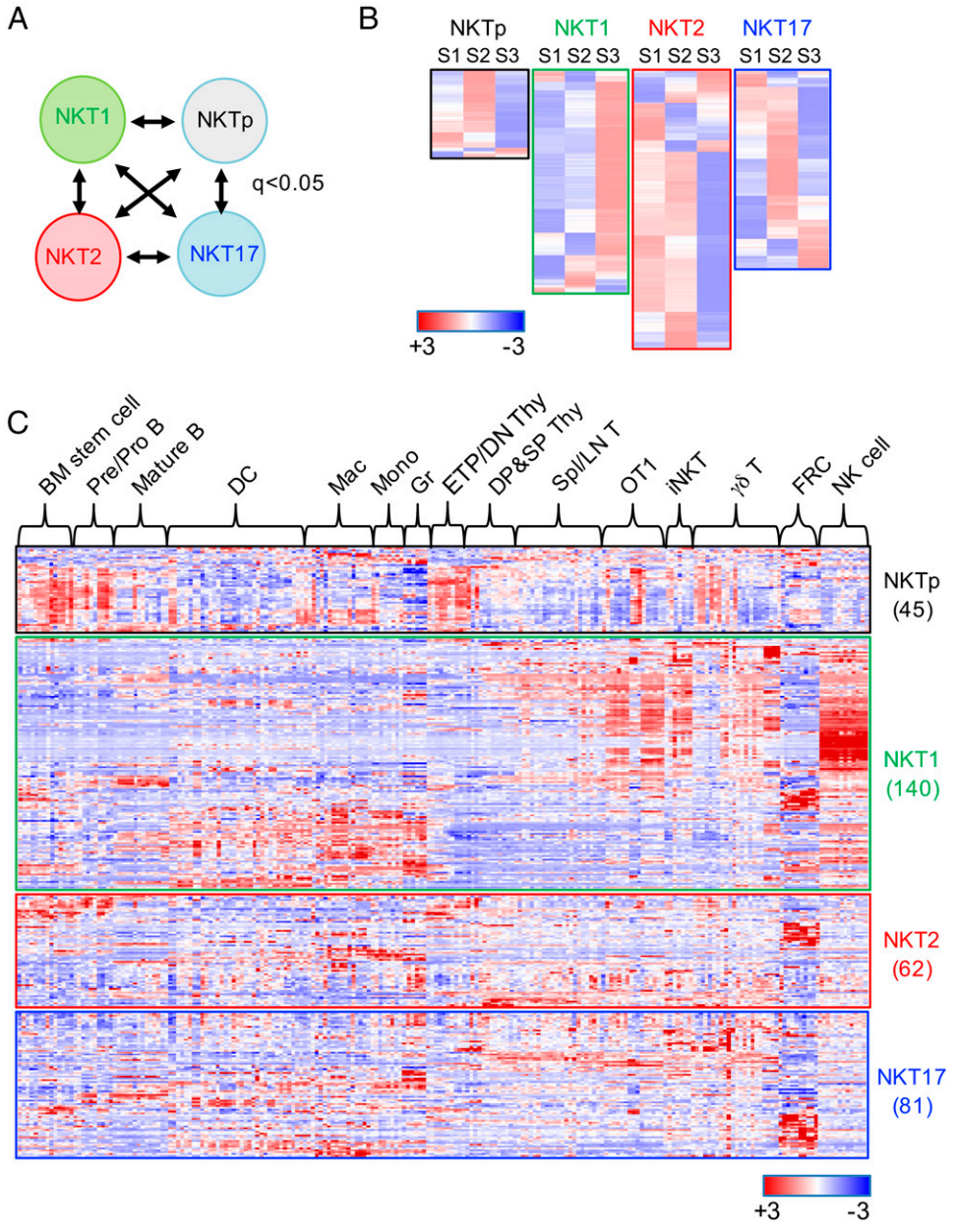

FIGURE 3. Only NKT1 cells share a transcriptional program with NK cells. (**A**) Schematic figure showing a comparison method to generate signature genes based on q values. (**B**) Expression pattern of signature genes of each iNKT subset was determined in each stage using ImmGen data set. (**C**) Expression profiles of signature genes of each iNKT subset were analyzed in hematopoietic cells using an Immunological Genome Project data set (accession number GSE15907), which encompassed 214 different hematopoietic lineages. Numbers in parentheses indicate the number of signature genes of each iNKT subset and detailed ImmGen cell type description is shown in Supplemental Fig. 1. BM, bone marrow; DC, dendritic cell; DN, double-negative; DP, double-positive; ETP, early thymic precursor; FRC, fibroblastic reticular cells; Gr, granulocyte; LN, lymph node; Mac, macrophage; Mono, monocyte; SP, single-positive; Spl, spleen; Thy, thymocytes.

consortium (8) (Fig. 3B). NKT1 signature genes were most highly expressed on stage 3 cells, NKTp and NKT17 signature genes were mainly on stage 2 cells, and NKT2 signature genes were present in both stage 1 and stage 2 cells. These features are consistent with previous reconciliation between conventional stages and functional subsets of iNKT cells in C57BL/6NCr mice (3, 4) and highlight that CD44 and NK1.1 are not accurate markers of developmental progression, but include mixed populations with developmental progenitor and terminal effector properties, particularly for stage 2. Next, we analyzed expression patterns of iNKT signature genes among various hematopoietic cells using ImmGen data that encompass 214 different cell types (Fig. 3C, detailed map in Supplemental Fig. 1). Previously, NKT cells were suggested to strongly share a transcriptional program with NK cells and that this core effector program was also shared with activated OT-1 CD8 T cells, intraepithelial γδ T cells, and early thymic precursors (ETP) (8). Our NKT1 signature genes were highly expressed in these cells too, except ETP (Fig. 3C). Instead, NKTp signature genes were enriched in ETP and other developing thymocytes and also highly shared among bone marrow stem cells, pre/pro-B cells, germinal center B cells, thymic dendritic cells, bone marrow macrophages, monocytes, OT-1 T cells within 48 h of activation, and $CD24^{hi}$ or fetal thymic γδ T cells (Supplemental Fig. 1). Thus, the extent to which the previous analysis showed iNKT similarity to ETP might have reflected the contamination of their population with progenitor cells. We reasoned that NKTp cells are often proliferating, and IPA showed *Myc*-associated genes were significantly enriched in NKTp cells ($p = 5.12 \times 10^{-6}$), followed by E2F, TP53, and RB1 (Table I). Because Myc regulates gene expression via complex means (15), we wanted to determine if the Myc-associated genes in NKTp were directly regulated by Myc. Thus, we analyzed a previous Myc-Chip seq dataset of activated mouse CD4 T cells (GSE37229) (16). Among the NKTp unique Myc-associated genes (Table I), EIF4A1, SLC2A1, and TFDP1 were within 1 kb of a direct Myc binding site, suggesting Myc directly regulate these genes. UTX was 12 Mbp away from the nearest Myc binding site, and the other six genes were from 20 to 500 kb apart. As Myc binds to promoters rather than enhancers (15, 16), these seven genes are more likely to be regulated indirectly by Myc. iNKT cell phenotype in the absence of Myc protein was analyzed previously, and indeed, the frequency of iNKT cells was greatly reduced (17, 18). In Myc-deficient mice, the number of $CD24^{hi}$ stage 0 NKT cells was normal, but development of iNKT cells was arrested at stage 1 or 2, indicating that positive selection from DP thymocytes was not affected. Thus, our findings are consistent with Myc-dependent cellular proliferation being a critical process for the development iNKT cells.

A second important observation is that only NKT1, but not NKTp, NKT2, or NKT17, cells showed transcriptional similarity to NK cells (Fig. 3C). Therefore, the previous conclusion that NKT cells have a hybrid nature between T cells and NK cells (8) is not correct, in that it only applies to a subset of NKT cells, albeit one that is particularly prominent in the C57BL/6 strain of mice. With the current ImmGen data set, we could not specify a type of lymphoid or myeloid cell overtly sharing transcripts with NKT2 and NKT17 cells (Fig. 3C). Overall, these results indicate that NKTp cells, as well as NKT1, NKT2, and NKT17 cells, are unique cells having distinctive transcriptional natures.

iNKT cells, Th CD4 cells, ILC, and γδ T cells share key transcripts

Not only iNKT cells, but also ILCs and γδ T cells, have effector subsets producing distinct effector cytokine analogous to conventional Th cells (9, 19, 20). However, it has not been addressed if these effector subsets share a common transcriptional nature or not, and to address this issue, we compared our dataset with published ones (7, 9, 10). The transcriptional nature of Th cells was analyzed using RNAseq of in vitro–differentiated naive CD4 T cells stimulated with anti-CD3/CD28 and cytokines (10), and ILC and γδ T cells were analyzed by microarray in previous ImmGen projects using cells that were sorted immediately ex vivo (7, 9). These four different datasets, however, used different analysis platforms, and it was not possible to make direct comparisons with each other. Thus, to gain insight into potential common effector programs, we first defined a short list of genes uniquely expressed in each iNKT subset and analyzed their expression patterns in Th cells, ILCs, and γδ T cells (Fig. 4A). These genes were enriched in each analogous subset of Th cells and ILCs, and NK cells, which were largely indistinguishable from ILC1s (7), were like NKT1 cells. Among various γδ T subsets, V gene usage correlates with distinct effector programs (9, 20). Based on published analysis (9), we identified V5 (intraepithelial $V\gamma5^{+}$), V6 (thymic $CD24^{low}$ $V\delta6^{+}$), and V2 (thymic $CD24^{low}$ $V\gamma2^{+}$) γδ T cells as sharing key effector genes with NKT1, NKT2, and NKT17 cells, respectively (Fig. 4A). Interestingly, $CD24^{hi}$ or fetal-derived γδ T subsets shared NKTp signature genes (Fig. 4B), suggesting that they may be a functional counterpart of NKTp cells. Overall, these features show iNKT and γδ T cells share effector differentiation programs and signature genes with analogous ILC and Th cells.

Overlapping signature genes define core transcriptional elements

Next, we identified signature genes of 13 different cell types from four different types of lymphoid cells as depicted in Fig. 4C by

Table I. List of upstream regulators of NKTp

Upstream Regulator	*p* Value of Overlap	Target Molecules in Dataset
MYC	5.12E-06	CCNB1, ECM1, EIF2B1, EIF4A1, LDHB, NDUFS4, SLC2A1, STMN1, TFDP1, UXT
E2F4	3.50E-05	GMNN, PTTG1, RPA3, STMN1, UXT
E2f	5.68E-05	CCNB1, GMNN, RPA3, UXT
E2F1	8.10E-05	CCNB1, GMNN, RPA3, STMN1, TAF9, UXT
NDUFA13	2.15E-04	CCNB1, TFDP1
CD 437	3.85E-04	EIF4A1, HMGN2, LSM3, UXT
TP53	4.20E-04	CCNB1, EIF2B1, GMNN, HMGN2, PTTG1, SLC2A1, SPC25, STMN1, TFDP1
NRAS	4.31E-04	CCNB1, SLC2A1, SPC25
RBL2	5.92E-04	CCNB1, STMN1, XT
AMPK	8.09E-04	CCNB1, LDHB, SLC2A1
MAPT	8.50E-04	ARF5, CCNB1, NDUFS4, STMN1
RB1	9.28E-04	CCNB1, GMNN, TFDP1, UXT

Upstream regulators of NKTp cells were generated using IPA, and list shows those with *p* value <0.0001.

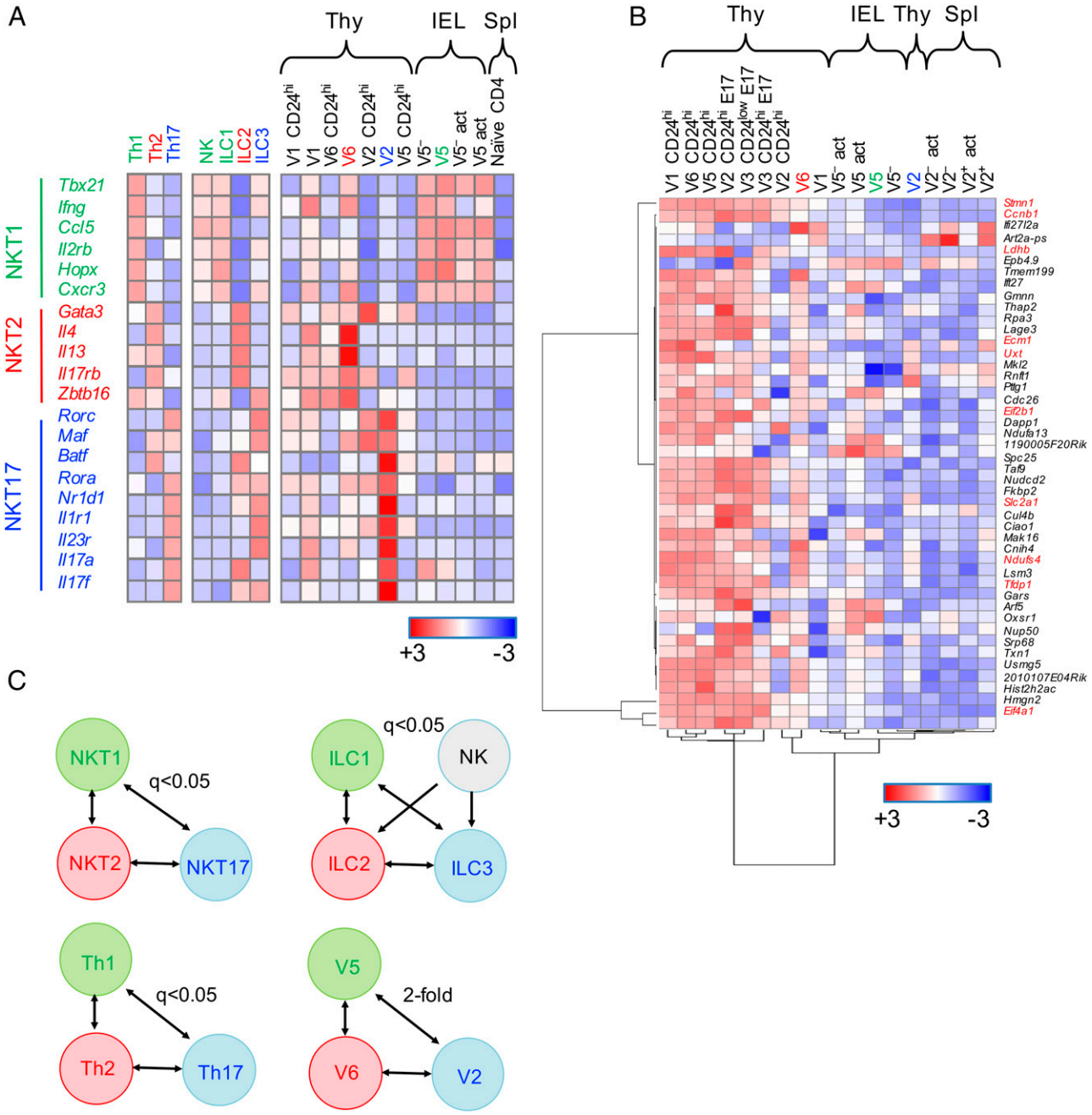

FIGURE 4. iNKT cells, Th cells, ILCs, and γδ T cells share key transcripts for each subset. (**A**) Genes highly expressed on NKT1 (green), NKT2 (red), and NKT17 (blue) cells were analyzed for their expression patterns in other analogous lymphoid lineages. (**B**) NKTp unique genes were analyzed for their expression pattern in various γδ T cell subsets. *Myc*-associated genes among NKTp signatures are highlighted in red. (**C**) Schematic figures show comparison methods of defining signature genes in each lineage. V1 (Vγ1$^+$), V2 (Vγ2$^+$), V3 (Vγ3$^+$), V5 (Vγ5$^+$), and V6 (Vδ6$^+$) represent γδ T cells. act, activated (CD44^{hi}); E17, embryonic day 17; IEL, intraepithelial lymphocytes, Spl, spleen; Thy; thymus.

doing intragroup differential gene expression comparison (Supplemental Table I). Then, we grouped IFN-γ–, IL-4–, and IL-17–secreting effector subsets cells, referring to them as L1, L2, and L3, respectively, and calculated the number of signature genes overlapping with each other (Fig. 5A). In the L1 group, we found 12 signature genes commonly shared among all subsets and 3 and 9 genes in the L2 and L3 groups, respectively. The L1 group was marked by effector cytokines or chemokines such as RANTES (encoded by *Ccl5*), granzyme B (encoded by *Gzmb*), and Perforin 1 (encoded by *Prf1*). IL-4 (encoded by *Il4*) and the IL-25R (encoded by *Il17rb*) were shared by all L2 subsets, suggesting a central role for IL-25 signaling. Consistent with this, development and/or expansion of IL-4–producing NKT2 cells and ILC2s were dependent on IL-25 (21, 22). We identified membrane-bound *O*-acetyltransferase1 (Mboat1 encoded by *Mboat1*), an enzyme involved in fatty acid metabolism (23), as a novel candidate for L2 function. L3 subsets shared RORγt (encoded by *Rorc*) and its known target molecules such as IL-1R1 (encoded by *Il1r1*) and IL-23R (encoded by *Il23r*) (24). Rev-Erb (encoded by *Nr1d1*) is a previously identified upstream molecule of RORγt, which mediates circadian rhythm (25). Syndecan-1 (encoded by *Sdc1*) is a known regulator of NKT17 cells (26), and IL-17RE (encoded by *Il17re*) is a receptor for IL-17C and important for Th17 cell activation (27). *Tmem176b* was previously detected as a putative RORγt binding partner (24), and we identified

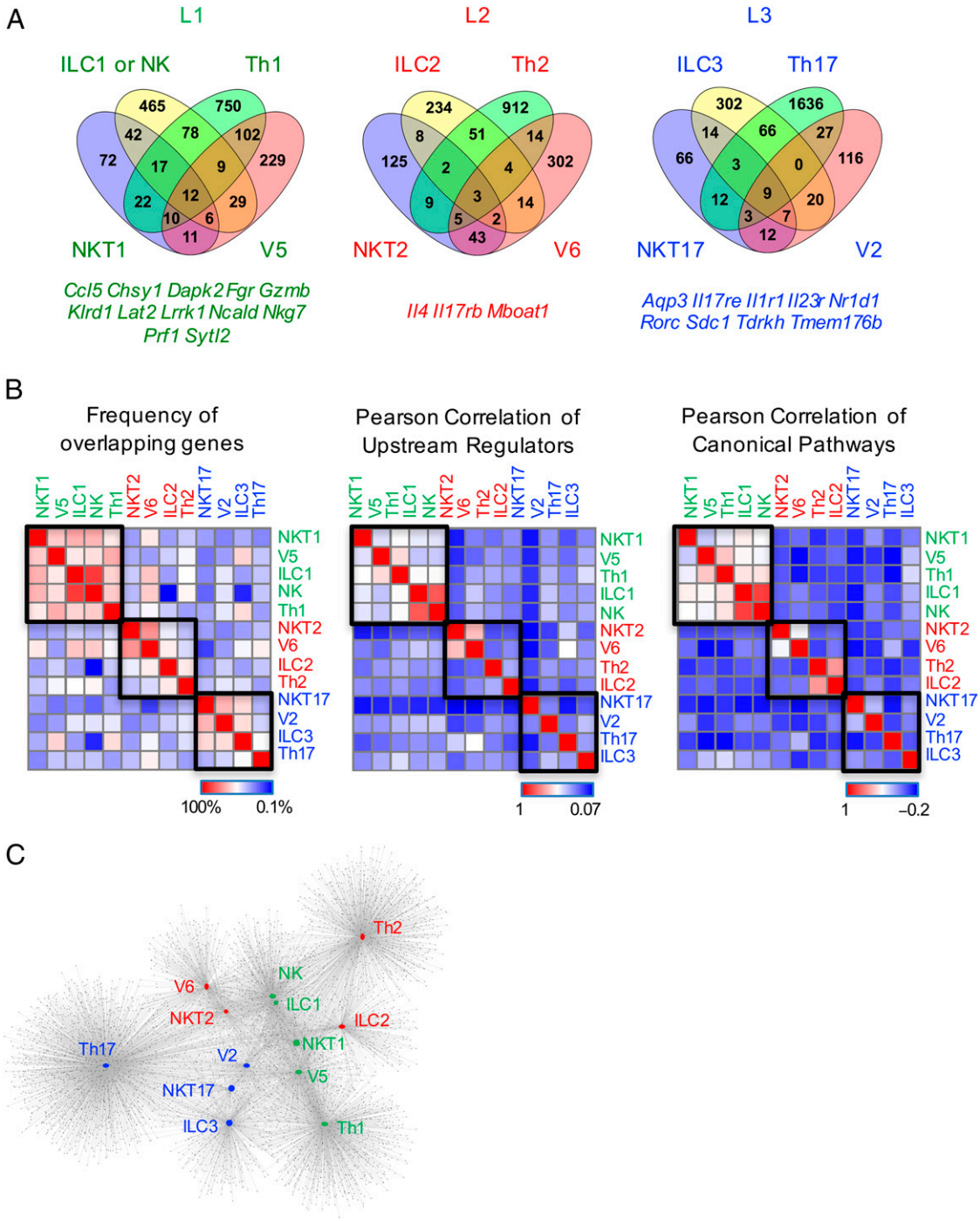

FIGURE 5. Overlapping signature genes define core transcriptional elements. (**A**) Venn diagrams show number of overlapping signature genes between subsets in each group. Genes shared by all subsets in each group are listed below each diagram. (**B**) Heat map shows frequency of overlapping genes and Pearson correlation of enrichment scores of upstream regulators and canonical pathways between two subsets. Data were log2-transformed and visualized by global expression. (**C**) Network analysis of signature genes. Each dot represents a single gene connected to subsets expressing them. V2 (Vγ2$^+$) and V6 (Vδ6$^+$) are thymic CD24^{low} $\gamma\delta$ T cells, and V5 (Vγ5$^+$) is intraepithelial $\gamma\delta$ T cells. Green: IFN-γ–producing cells; red: IL-4–producing cells; blue: IL-17–producing cells.

two additional candidates common to all L3 subsets; Aquaporin 3 (encoded by *Aqp3*), which is a water channel transporting hydrogen peroxide and required for T cell migration and IL-23–dependent skin inflammation (28, 29), and tudor and KH domain containing (encoded by *Tdrkh*), which is essential for spermatogenesis and piwi-interacting RNA biosynthesis (30). *Tbx21* and *Ifng* were not detected as shared signatures of L1 lineage because some ILC3s are derived from ILC1 (31), and these genes remain transcriptionally active in them (Fig. 4A). As GATA3 was highly expressed in both NKT2 and NKT17 cells, and L3 subsets were not transcriptionally active for IL-17 at steady state, these two genes were not identified as common lineage signatures.

Next, we sought to visualize the relatedness of the transcriptomes of different subsets. After pairwise comparison within groups, we generated a heat map showing the frequencies of overlapping signature genes between any two cell types among all 13 different subsets. Whereas L1 subsets highly shared their signature genes with each other, Th2 in L2 and Th17 in L3 groups had less sharing among signature genes (Fig. 5B, left panel). This feature was also visualized in network analysis (Fig. 5C), in which each

Table II. NES and FDR of gene set enrichment analysis

	NKT1 > NKT2		NKT1 > NKT17		NKT2 > NKT17		
Category	NES	FDR	NES	FDR	NES	FDR	Correlation
iNKT							
NKT1	7.36	0	6.95	0	0	NA	NKT1
NKT2	−8.03	0	0	NA	7.19	0	NKT2
NKT17	0	NA	−8.2	0	−7.5	0	NKT17
CD4 T							
Th1	4.2	0	3.15	0	1.4	0.1	NKT1
Th2	−0.7	0.83	0.79	0.75	−1.29	0.15	No correlation
Th17	−2.89	0	−2.4	0	−1.5	0.06	NKT17 > NKT2 > NKT1
NK and ILC							
NK	4.43	0	4.67	0	1.29	0.17	NKT1
ILC1	4.4	0	4.18	0	2.1	0.002	NKT1 > NKT2 > NKT17
ILC2	−2.9	0	−1.1	0.29	1.5	0.08	NKT2 > NKT17 > NKT1
ILC3	1.5	0.07	−3.6	0	−4.6	0	NKT17
γδ T							
V5	4.27	0	4.0	0	−0.73	.82	NKT1
V6	−4.68	0	2.22	0.004	5.05	0	NKT2 > NKT1 > NKT17
V2	2.28	0	−4.59	0	−5.28	0	NKT17 > NKT1 > NKT2
V1	1.79	0.01	1.58	0.04	−1.1	0.33	NKT1

V1 ($V\gamma1^+V\delta6^-$), V2 ($V\gamma2^+$), and V6 ($V\delta6^+$) are thymic $CD24^{low}$ γδ T cells and V5 ($V\gamma5^+$) is intraepithelial γδ T cells.
NA, not applicable.

dot indicates a single gene with a line connecting to cells expressing them, and the distance between subsets is proportional to the number of interconnected overlapping genes. In this analysis, L1 subsets were all grouped together, whereas L2 and L3 subsets were more separated. V2, NKT17, and ILC3 cells were closely grouped, but equidistant between Th1 and Th17 cells, indicating Th17 cells do not share more genes in common with other L3 subsets than Th1 cells share with them (Fig. 5C). NKT2 and V6 were close, but they were grouped closer to Th17 than Th2 cells.

The tighter clustering of L1 subsets compared with L2 or L3 subsets was also reflected in upstream regulators and canonical pathway enrichment analysis (Supplemental Table II). We generated heat maps showing Pearson correlation of enrichment score of each upstream regulator and canonical pathway, in which the L1 group shared more common components than L2 and L3 groups (Fig. 5B, middle and right panels). Among canonical pathways, L1 shared 22, including the strongly enriched NK cell signaling pathway. L2 and L3 did not share a single common one, though we listed the pathways shared among three out of four subsets of L2 and L3 groups (Supplemental Table II). Of interest, the pathways cAMP and protein kinase A signaling were shared among L2 cell types, perhaps suggesting an important role for adenosine. Other pathways such as airway inflammation in asthma were shared among L2 cell types except Th2, and type 1 diabetes mellitus signaling was shared among L3 cell types except V2. Collectively, these features indicate each lymphoid lineage (L1, L2, and L3) shares key cytokines, transcriptional elements, canonical pathways, and upstream regulators, but the overall signature genes of innate lymphoid or innate-like T cells are less shared with the analogous Th cells, especially Th2 and Th17 cells.

iNKT subsets are more closely related to innate lymphocytes than to conventional Th cells

The analysis of overlapping signature genes (Fig. 5B, 5C) indicated that there is substantial heterogeneity among subsets within each lymphoid lineage. To quantify the transcriptional similarities of iNKT subsets with other lymphoid lineages, we performed multiple rounds of gene set enrichment analysis (Supplemental Fig. 2). In this analysis, the differentially expressed genes of each subset of Th cells, ILCs, and γδ T cells were aligned on lists of genes differentially expressed between iNKT subsets. By measuring NES, we quantitatively determined how significantly one subset shares a transcriptome with one of the iNKT subsets. For example, NK signature genes were highly enriched in NKT1 compared with both NKT2 and NKT17 cells (Supplemental Fig. 2B). Table II shows NES scores and false discovery rate (FDR) of all comparisons and the abbreviated interpretation (correlation column). As a result, signature genes of Th1, ILC1, NK, and V5 were all highly enriched in NKT1 cells compared with NKT2 and NKT17 cells, indicating L1 lymphoid cells are transcriptionally similar. Unexpectedly, Th2 signature genes had no skewing toward any of the iNKT subsets, whereas ILC2 and V6 signature genes were enriched in NKT2 cells (Supplemental Fig. 2). Similarly, Th17 signature genes were not strongly enriched in NKT17 cells, unlike ILC3 and V2 cells. Again, to visualize these trends, we plotted NES scores as x, y, and z coordinates, respectively (Table II), plotted them into three different two-dimensional coordinates, and grouped together cells having NKT1 (green), NKT2 (red), or NKT17 (blue) nature (Fig. 6A). We used the NES value of each iNKT subset signatures as a positive control and finally measured distance from the positive control to each cell type to measure relative distance (Fig. 6B). All L1 subgroups were closer to NKT1 cells than NKT2 and NKT17 cells, but NKT2 and NKT17 cells were more likely to be analogous to γδ or ILC subsets than Th subsets. Th2 signature genes had similar distance from all three subsets of iNKT cells, and Th17 signature genes marginally separated NKT17 cells from NKT2 cells. These features quantitatively show that the transcriptional profiles of iNKT subsets are most closely related to γδ T cells and ILCs, whereas CD4 Th cells had the least similarities.

Discussion

In this report, we describe the transcriptional nature of iNKT subsets using RNA sequencing. Our analysis revealed that NKTp cells have a dramatically distinct transcriptional program compared with all other iNKT effector subsets, even NKT2 cells (which are largely phenotypically indistinguishable from NKTp). This progenitor program was enriched in *Myc*-regulated genes, consistent with rapid proliferation, which is known to characterize NKT development, and does not occur with conventional T cells at the analogous stage of development (17, 18). These data should allow for the identification of better markers to experimentally distinguish NKTp from mature NKT effector cells, a matter that we are currently investigating.

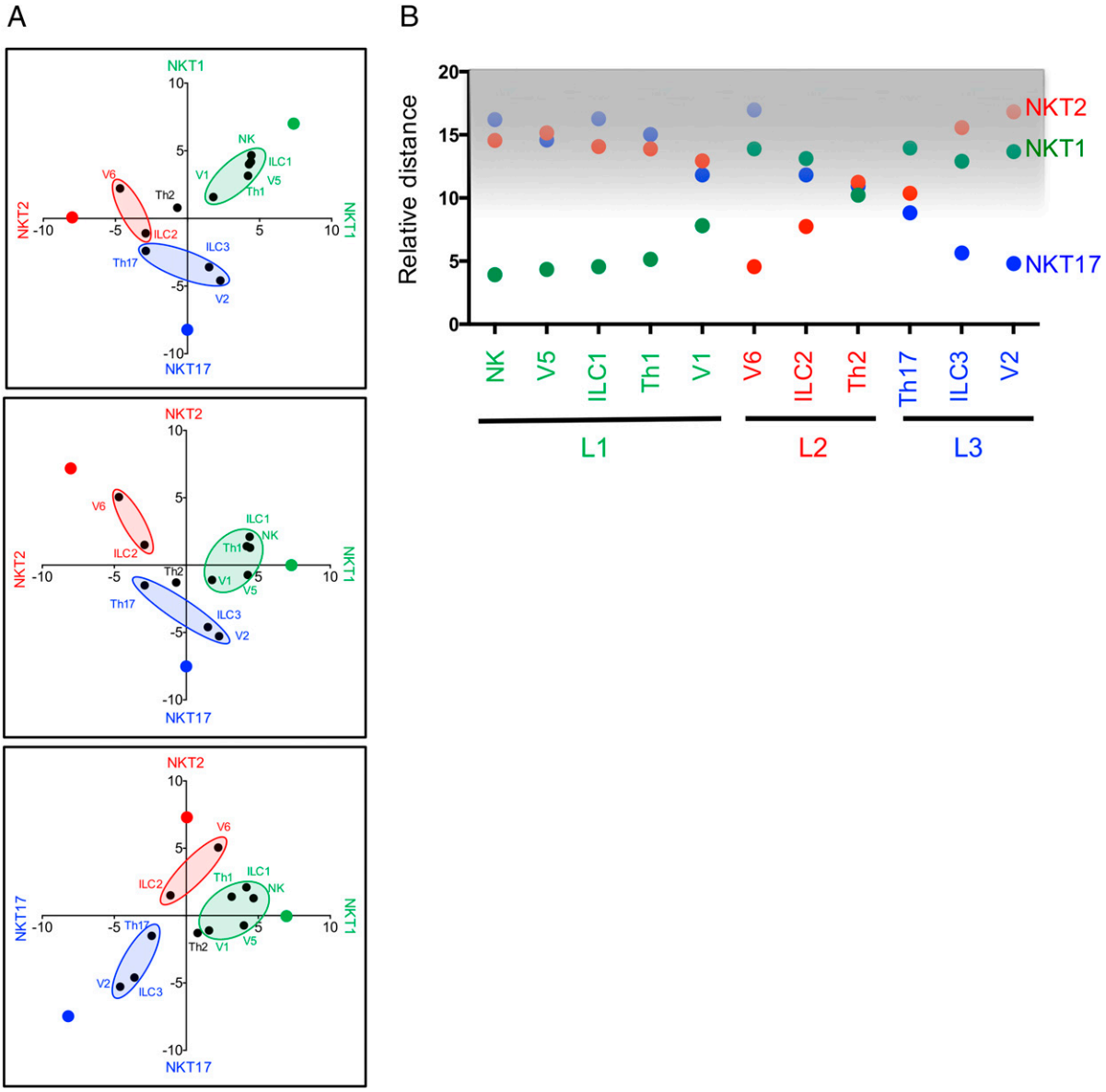

FIGURE 6. iNKT subsets are more closely related to innate lymphocytes than to conventional Th cells. (**A**) NES values (Table I) were regarded as x, y, and z coordinates and plotted in three different axis combinations. Each dot represents labeled population, and green, red, and blue dots without label represent NES of NKT1, NKT2, and NKT17 signature genes, respectively. (**B**) Relative distance was defined as an arbitrary length between two populations from (A). V2 (Vγ2$^+$) and V6 (Vδ6$^+$) are thymic CD24^{low} γδ T cells, and V5 (Vγ5$^+$) is intraepithelial γδ T cells.

We also compared our data to published data sets including Th cells, ILCs, and γδ T cells and showed that the transcriptional nature of NKT subsets are most like the analogous subsets of γδ T cells, followed by ILCs. Th1 CD4 T cells were similar to NKT1 cells, but Th2 and Th17 cells did not show high similarity to other L2 and L3 subsets. Overall, this study indicates that innate or innate-like T cells share a common transcriptional nature distinct from adaptive Th cells. PLZF is a transcription factor directing innate function of iNKT cells (32, 33), and 50–70% of ILCs were derived from bone marrow stem cells that once expressed PLZF (34). Previous reports showed that V6 and V2 cells express PLZF, and we also found V5 cells express more abundant PLZF transcripts than naive splenic CD4 T cells (Fig. 4A). In conventional Th cells, however, PLZF expression was stably suppressed and not induced by TCR signaling or inflammatory milieu (35). Therefore, PLZF may be one of key transcriptional elements regulating the common nature of ILC and innate-like T cells. One caveat to the interpretation of these data is that the Th cells were in vitro generated, whereas other cells were directly isolated from in vivo (10). Furthermore, it is unclear whether the differences between gene expression profiles of some Th subsets and their innate counterparts is a consequence of the fact that conventional T cells are analyzed relatively soon after polarization, whereas the innate immune populations may have been in their functional differentiation states for longer. Two recently published papers came to a similar conclusion as ours, showing directly isolated human ILC and Th subsets are transcriptionally distinct (36), and mouse in vivo Th2 cells acquired part of, but not all of, ILC2 regulomes upon infection (37). In contrast, the striking similarities between Th1 and IFN-γ–producing innate immune cells indicate that gene expression by in vitro Th1 polarization closely matches that of in vivo–differentiated NKT1, NK, V5, and ILC1 populations.

A previous report showed there are three functionally distinct γδ T cell subsets that develop in the thymus; V1, V6, and V2 cells (9, 20). In our analysis, however, V1 cells were not clearly categorized as similar to one or more of the iNKT subsets (Fig. 4A),

although they had a weak NKT1 nature (Fig. 6, Table II). Instead, we showed intraepithelial γδ T cells corresponded strongly to NKT1 cells and used V5 as a representative among four different subsets (Fig. 4A). As a result, we found V5, V6, and V2 cells were analogous to NKT1, NKT2, and NKT17 cells, respectively. Abundance of PLZF transcripts in γδ T cell subsets was also analogous to iNKT subsets—high in V6, intermediate in V2 and low in V5 (Fig. 4A). In the absence of PLZF, V6 and Vγ4$^+$ γδ T cells, which are similar to V2 cells, failed to produce cytokines upon stimulation (38, 39), suggesting PLZF is required for functional maturation of these cells. Further study is required to clarify how Ag receptor specificity and transcription factors direct functional heterogeneity of γδ T cells.

Mucosal-associated invariant T (MAIT) cells are a specialized type of T cells recognizing riboflavin (vitamin B2) metabolites in the context of MR1 (40). They have limited T cell diversity in both mice and humans, and a recent report using MR1 tetramers showed that they all express PLZF and are dependent on it for development (41). In addition, MAITs had subsets expressing TBET and RORγt among the MR1 tetramer-positive cells (41), suggesting the possibility that effector differentiation profiles of MAITs might also be analogous to iNKT cells. Future studies will be required to analyze their genetic nature in a subset-dependent manner.

In summary, we showed that the four different subsets of iNKT cells are transcriptionally unique and identified NKTp as a distinct entity regulated by the Myc-dependent signaling. With comprehensive comparison analyses, we found the developmental profiles of iNKT subsets were more similar to those of γδ T cells or ILCs than to conventional Th cells and identified core genes showing highest association with each lymphoid effector lineage.

Disclosures

The authors have no financial conflicts of interest.

References

1. Bendelac, A., P. B. Savage, and L. Teyton. 2007. The biology of NKT cells. *Annu. Rev. Immunol.* 25: 297–336.
2. Egawa, T., G. Eberl, I. Taniuchi, K. Benlagha, F. Geissmann, L. Hennighausen, A. Bendelac, and D. R. Littman. 2005. Genetic evidence supporting selection of the Valpha14i NKT cell lineage from double-positive thymocyte precursors. *Immunity* 22: 705–.
3. Lee, Y. J., K. L. Holzapfel, J. Zhu, S. C. Jameson, and K. A. Hogquist. 2013. Steady-state production of IL-4 modulates immunity in mouse strains and is determined by lineage diversity of iNKT cells. *Nat. Immunol.* 14: 1146–1154.
4. Constantinides, M. G., and A. Bendelac. 2013. Transcriptional regulation of the NKT cell lineage. *Curr. Opin. Immunol.* 25: 161–167.
5. Mohrs, K., A. E. Wakil, N. Killeen, R. M. Locksley, and M. Mohrs. 2005. A two-step process for cytokine production revealed by IL-4 dual-reporter mice. *Immunity* 23: 419–429.
6. Lee, Y. J., H. Wang, G. J. Starrett, V. Phuong, S. C. Jameson, and K. A. Hogquist. 2015. Tissue-Specific Distribution of iNKT Cells Impacts Their Cytokine Response. *Immunity* 43: 566–578.
7. Robinette, M. L., A. Fuchs, V. S. Cortez, J. S. Lee, Y. Wang, S. K. Durum, S. Gilfillan, and M. Colonna, Immunological Genome Consortium. 2015. Transcriptional programs define molecular characteristics of innate lymphoid cell classes and subsets. *Nat. Immunol.* 16: 306–317.
8. Cohen, N. R., P. J. Brennan, T. Shay, G. F. Watts, M. Brigl, J. Kang, and M. B. Brenner, Immunological Genome Project Consortium. 2013. Shared and distinct transcriptional programs underlie the hybrid nature of iNKT cells. *Nat. Immunol.* 14: 90–99.
9. Narayan, K., K. E. Sylvia, N. Malhotra, C. C. Yin, G. Martens, T. Vallerskog, H. Kornfeld, N. Xiong, N. R. Cohen, M. B. Brenner, et al; Immunological Genome Project Consortium. 2012. Intrathymic programming of effector fates in three molecularly distinct γδ T cell subtypes. *Nat. Immunol.* 13: 511–518.
10. Stubbington, M. J., B. Mahata, V. Svensson, A. Deonarine, J. K. Nissen, A. G. Betz, and S. A. Teichmann. 2015. An atlas of mouse CD4(+) T cell transcriptomes. *Biol. Direct* 10: 14.
11. Kim, D., G. Pertea, C. Trapnell, H. Pimentel, R. Kelley, and S. L. Salzberg. 2013. TopHat2: accurate alignment of transcriptomes in the presence of insertions, deletions and gene fusions. *Genome Biol.* 14: R36.
12. Trapnell, C., A. Roberts, L. Goff, G. Pertea, D. Kim, D. R. Kelley, H. Pimentel, S. L. Salzberg, J. L. Rinn, and L. Pachter. 2012. Differential gene and transcript expression analysis of RNA-seq experiments with TopHat and Cufflinks. *Nat. Protoc.* 7: 562–578.
13. Subramanian, A., P. Tamayo, V. K. Mootha, S. Mukherjee, B. L. Ebert, M. A. Gillette, A. Paulovich, S. L. Pomeroy, T. R. Golub, E. S. Lander, and J. P. Mesirov. 2005. Gene set enrichment analysis: a knowledge-based approach for interpreting genome-wide expression profiles. *Proc. Natl. Acad. Sci. U S A* 102: 15545–15550.
14. Shannon, P., A. Markiel, O. Ozier, N. S. Baliga, J. T. Wang, D. Ramage, N. Amin, B. Schwikowski, and T. Ideker. 2003. Cytoscape: a software environment for integrated models of biomolecular interaction networks. *Genome Res.* 13: 2498–2504.
15. Levens, D. 2013. Cellular MYCro economics: Balancing MYC function with MYC expression. [Published erratum appears in 2013 Cold Spring Harb. Perspect. Med. 3: a022483.] *Cold Spring Harb. Perspect. Med.* 3: 3.
16. Nie, Z., G. Hu, G. Wei, K. Cui, A. Yamane, W. Resch, R. Wang, D. R. Green, L. Tessarollo, R. Casellas, et al. 2012. c-Myc is a universal amplifier of expressed genes in lymphocytes and embryonic stem cells. *Cell* 151: 68–79.
17. Dose, M., B. P. Sleckman, J. Han, A. L. Bredemeyer, A. Bendelac, and F. Gounari. 2009. Intrathymic proliferation wave essential for Valpha14+ natural killer T cell development depends on c-Myc. *Proc. Natl. Acad. Sci. U S A* 106: 8641–8646.
18. Mycko, M. P., I. Ferrero, A. Wilson, W. Jiang, T. Bianchi, A. Trumpp, and H. R. MacDonald. 2009. Selective requirement for c-Myc at an early stage of V(alpha)14i NKT cell development. *J. Immunol.* 182: 4641–4648.
19. De Obaldia, M. E., and A. Bhandoola. 2015. Transcriptional regulation of innate and adaptive lymphocyte lineages. *Annu. Rev. Immunol.* 33: 607–642.
20. Kang, J., and N. Malhotra. 2015. Transcription factor networks directing the development, function, and evolution of innate lymphoid effectors. *Annu. Rev. Immunol.* 33: 505–538.
21. Watarai, H., E. Sekine-Kondo, T. Shigeura, Y. Motomura, T. Yasuda, R. Satoh, H. Yoshida, M. Kubo, H. Kawamoto, H. Koseki, and M. Taniguchi. 2012. Development and function of invariant natural killer T cells producing T(h)2- and T(h)17-cytokines. *PLoS Biol.* 10: e1001255.
22. von Moltke, J., M. Ji, H. E. Liang, and R. M. Locksley. 2016. Tuft-cell-derived IL-25 regulates an intestinal ILC2-epithelial response circuit. *Nature* 529: 221–225.
23. Hishikawa, D., H. Shindou, S. Kobayashi, H. Nakanishi, R. Taguchi, and T. Shimizu. 2008. Discovery of a lysophospholipid acyltransferase family essential for membrane asymmetry and diversity. *Proc. Natl. Acad. Sci. U S A* 105: 2830–2835.
24. Ciofani, M., A. Madar, C. Galan, M. Sellars, K. Mace, F. Pauli, A. Agarwal, W. Huang, C. N. Parkurst, M. Muratet, et al. 2012. A validated regulatory network for Th17 cell specification. *Cell* 151: 289–303.
25. Yu, X., D. Rollins, K. A. Ruhn, J. J. Stubblefield, C. B. Green, M. Kashiwada, P. B. Rothman, J. S. Takahashi, and L. V. Hooper. 2013. TH17 cell differentiation is regulated by the circadian clock. *Science* 342: 727–730.
26. Dai, H., A. Rahman, A. Saxena, A. K. Jaiswal, A. Mohamood, L. Ramirez, S. Noel, H. Rabb, C. Jie, and A. R. Hamad. 2015. Syndecan-1 identifies and controls the frequency of IL-17-producing naïve natural killer T (NKT17) cells in mice. *Eur. J. Immunol.* 45: 3045–3051.
27. Chang, S. H., J. M. Reynolds, B. P. Pappu, G. Chen, G. J. Martinez, and C. Dong. 2011. Interleukin-17C promotes Th17 cell responses and autoimmune disease via interleukin-17 receptor E. *Immunity* 35: 611–621.
28. Hara-Chikuma, M., S. Chikuma, Y. Sugiyama, K. Kabashima, A. S. Verkman, S. Inoue, and Y. Miyachi. 2012. Chemokine-dependent T cell migration requires aquaporin-3-mediated hydrogen peroxide uptake. *J. Exp. Med.* 209: 1743–1752.
29. Hara-Chikuma, M., H. Satooka, S. Watanabe, T. Honda, Y. Miyachi, T. Watanabe, and A. S. Verkman. 2015. Aquaporin-3-mediated hydrogen peroxide transport is required for NF-κB signalling in keratinocytes and development of psoriasis. *Nat. Commun.* 6: 7454.
30. Saxe, J. P., M. Chen, H. Zhao, and H. Lin. 2013. Tdrkh is essential for spermatogenesis and participates in primary piRNA biogenesis in the germline. *EMBO J.* 32: 1869–1885.
31. Spits, H., D. Artis, M. Colonna, A. Diefenbach, J. P. Di Santo, G. Eberl, S. Koyasu, R. M. Locksley, A. N. McKenzie, R. E. Mebius, et al. 2013. Innate lymphoid cells–a proposal for uniform nomenclature. *Nat. Rev. Immunol.* 13: 145–149.
32. Kovalovsky, D., O. U. Uche, S. Eladad, R. M. Hobbs, W. Yi, E. Alonzo, K. Chua, M. Eidson, H. J. Kim, J. S. Im, et al. 2008. The BTB-zinc finger transcriptional regulator PLZF controls the development of invariant natural killer T cell effector functions. *Nat. Immunol.* 9: 1055–1064.
33. Savage, A. K., M. G. Constantinides, J. Han, D. Picard, E. Martin, B. Li, O. Lantz, and A. Bendelac. 2008. The transcription factor PLZF directs the effector program of the NKT cell lineage. *Immunity* 29: 391–403.
34. Constantinides, M. G., B. D. McDonald, P. A. Verhoef, and A. Bendelac. 2014. A committed precursor to innate lymphoid cells. *Nature* 508: 397–401.
35. Zhang, S., A. Laouar, L. K. Denzin, and D. B. Sant'Angelo. 2015. Zbtb16 (PLZF) is stably suppressed and not inducible in non-innate T cells via T cell receptor-mediated signaling. *Sci. Rep.* 5: 12113.
36. Koues, O. I., P. L. Collins, M. Cella, M. L. Robinette, S. I. Porter, S. C. Pyfrom, J. E. Payton, M. Colonna, and E. M. Oltz. 2016. Distinct Gene Regulatory Pathways for Human Innate versus Adaptive Lymphoid Cells. *Cell* 165: 1134–1146.
37. Shih, H. Y., G. Sciumè, Y. Mikami, L. Guo, H. W. Sun, S. R. Brooks, J. F. Urban, Jr., F. P. Davis, Y. Kanno, and J. J. O'Shea. 2016. Developmental Acquisition of Regulomes Underlies Innate Lymphoid Cell Functionality. *Cell* 165: 1120–1133.

38. Chien, Y. H., X. Zeng, and I. Prinz. 2013. The natural and the inducible: interleukin (IL)-17-producing γδ T cells. *Trends Immunol.* 34: 151–154.
39. Kreslavsky, T., A. K. Savage, R. Hobbs, F. Gounari, R. Bronson, P. Pereira, P. P. Pandolfi, A. Bendelac, and H. von Boehmer. 2009. TCR-inducible PLZF transcription factor required for innate phenotype of a subset of gammadelta T cells with restricted TCR diversity. *Proc. Natl. Acad. Sci. U S A* 106: 12453–12458.
40. Kjer-Nielsen, L., O. Patel, A. J. Corbett, J. Le Nours, B. Meehan, L. Liu, M. Bhati, Z. Chen, L. Kostenko, R. Reantragoon, et al. 2012. MR1 presents microbial vitamin B metabolites to MAIT cells. *Nature* 491: 717–723.
41. Rahimpour, A., H. F. Koay, A. Enders, R. Clanchy, S. B. Eckle, B. Meehan, Z. Chen, B. Whittle, L. Liu, D. P. Fairlie, et al. 2015. Identification of phenotypically and functionally heterogeneous mouse mucosal-associated invariant T cells using MR1 tetramers. *J. Exp. Med.* 212: 1095–1108.

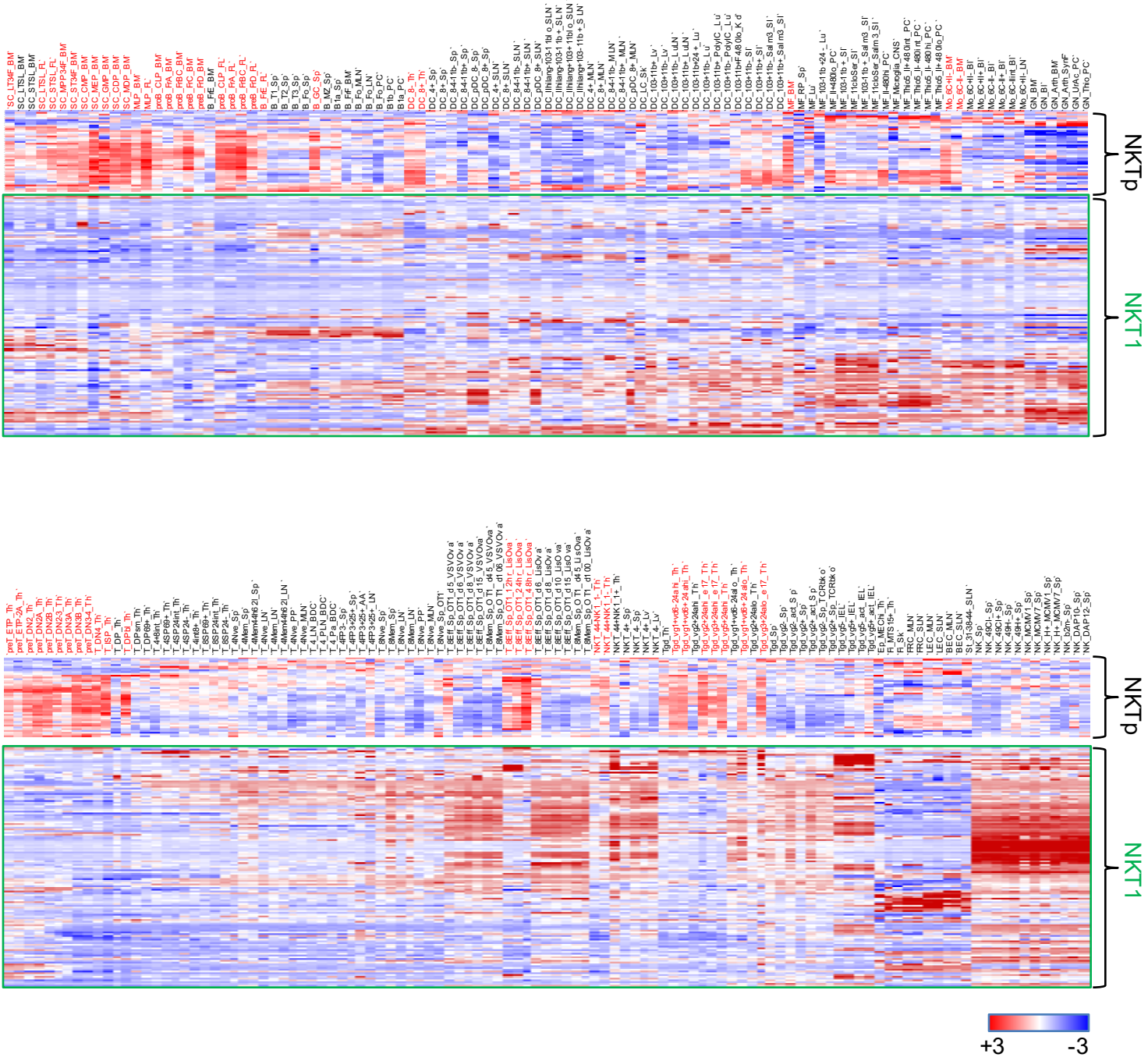

Supplemental Figure 1. NKTp unique transcripts are enriched in proliferating or differentiating hematopoietic cells. Signature genes of NKT progenitors (NKTp) and NKT1 cells were identified as shown in Fig. 3a and their expression patterns were analyzed across 214 different hematopoietic cells using ImmGen dataset. Each column was labeled as in ImmGen dataset and highlighted in red when NKTp signature genes were highly expressed.

A

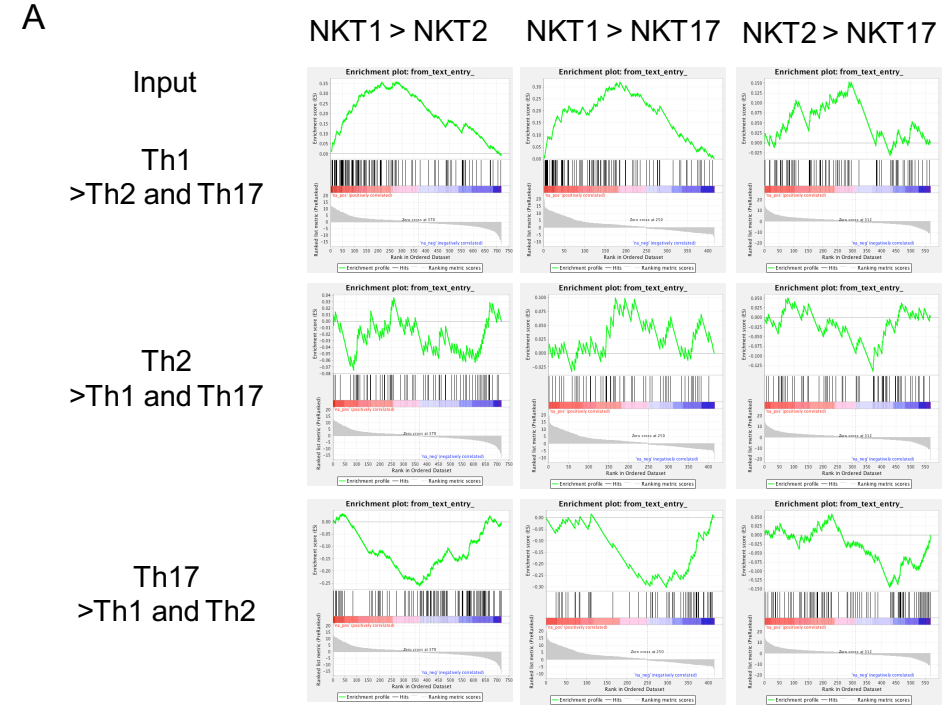
NKT1 > NKT2
NKT1 > NKT17
NKT2 > NKT17
Input
Th1 >Th2 and Th17
Th2 >Th1 and Th17
Th17 >Th1 and Th2

B

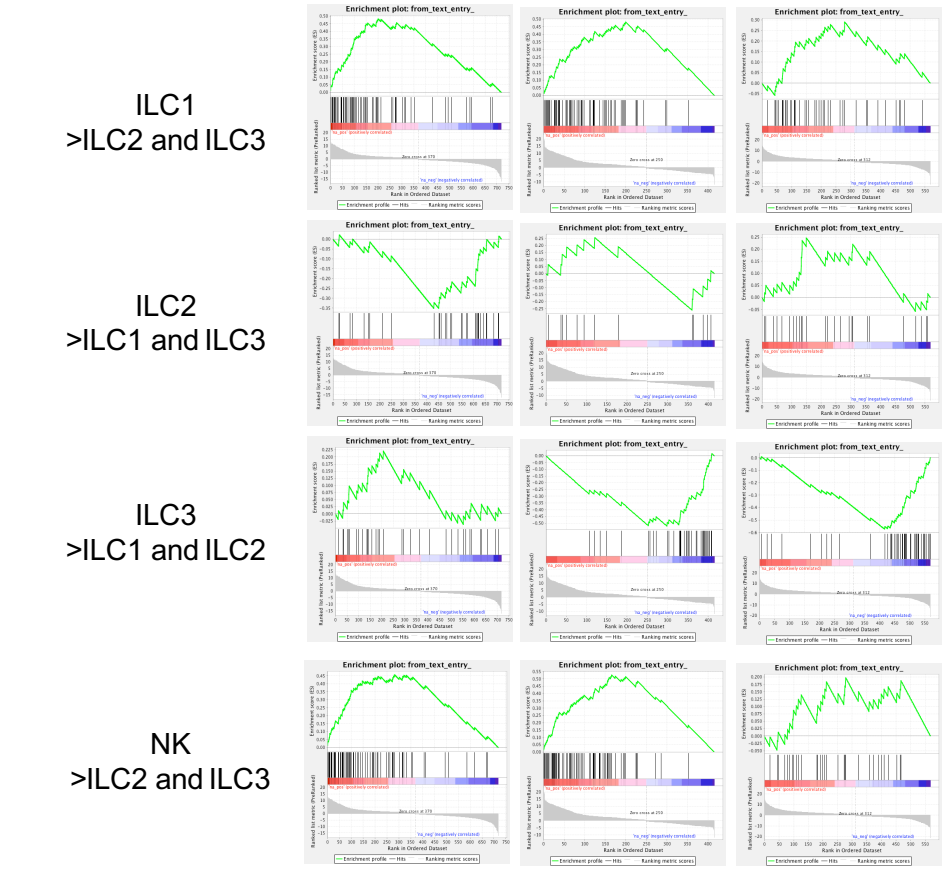
ILC1 >ILC2 and ILC3
ILC2 >ILC1 and ILC3
ILC3 >ILC1 and ILC2
NK >ILC2 and ILC3

C

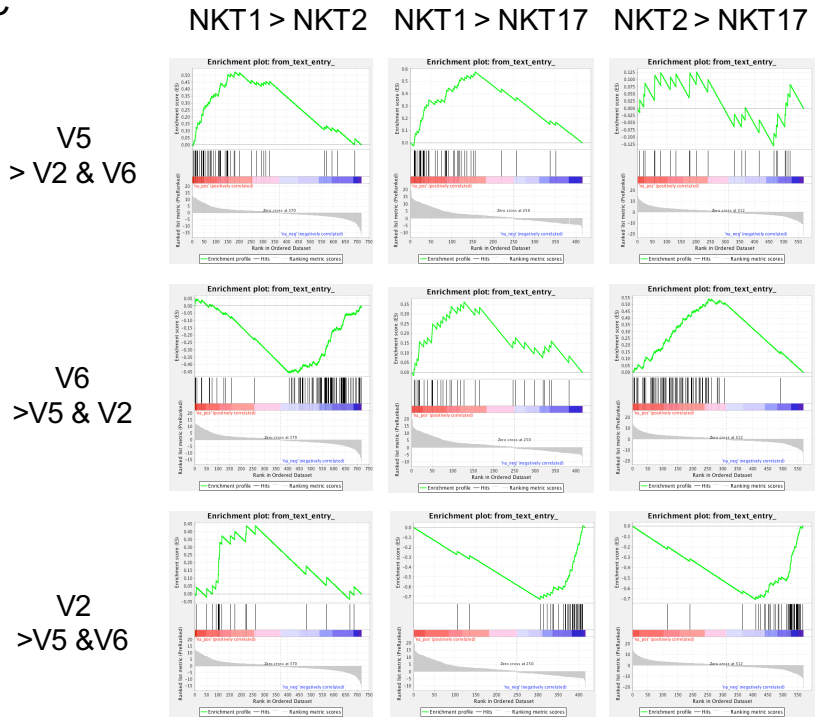

Supplemental Figure 2. Gene set enrichment analysis (GSEA). Signature genes of T helper cells (a), innate lymphoid cells (ILC) (b) and γδ T cells (c) were probed on genes differentially expressed between iNKT subsets. Subset signature genes were listed is Supplementary Table 1. V2 (Vγ2+) and V6 (Vδ6+) are thymic CD24^{low} cells γδ T cells and V5 (Vγ5+) is intraepithelial γδ T cells.

Supplementary Table 1. List of subset signature genes. Gene lists were generated as depicted in Fig. 3A and 4C.

NKT1	NKT2	NKT17	NKTp
>NKTp, NKT2 & NKT17	>NKTp, NKT1 & NKT17	>NKTp, NKT1 & NKT2	>NKT1, NKT2 & NKT17
140	**62**	**81**	**45**
1700026L06RIK	2610018G03RIK	1300014J06RIK	1190005F20RIK
1700128F08RIK	3830431G21RIK	2310007L24RIK	2010107E04RIK
2700097O09RIK	4930555I21RIK	ABI3BP	ARF5
4933440M02RIK	6330406I15RIK	ACPP	ART2A-PS
6330512M04RIK	ABHD13	ADD3	CCNB1
A430084P05RIK	ACP5	ADRB2	CDC26
ANXA2	ANO7	AGPAT5	CIAO1
APOL9B	APBB2	ANKRD6	CNIH4
ARL4D	ARHGAP20	APP	CUL4B
AW112010	ARMCX1	AQP3	DAPP1
BIN1	ATP1A3	ARL5C	ECM1
BTG2	BTLA	ARNT2	EIF2B1
CCDC136	C330018D20RIK	BLK	EIF4A1
CCL1	CDCA5	CACNA1A	EPB4.9
CCL4	CMTM4	CCDC86	FKBP2
CCL5	DEPDC1A	CD72	GARS
CCR8	DLEC1	CHAD	GMNN
CD160	DNM3	CORO2B	HIST2H2AC
CD2	DYRK4	CPE	HMGN2
CD244	E2F7	CREG1	IFI27L2A
CD63	F13A1	CRMP1	IFT27
CERCAM	FABP7	CRTAM	LAGE3
CHSY1	FAM169B	D17H6S56E-3	LDHB
CLDN12	FAM55B	DOCK5	LSM3
CLIC5	FAM71F2	ELMOD1	MAK16
CPNE7	FLRT2	EMB	MKL2
CRIM1	GATA1	F2R	NDUFA13
CSDA	GM129	FAM189A1	NDUFS4
CTLA2B	GM973	FAM83A	NUDCD2
CTSW	GPR97	FRMD6	NUP50
CX3CR1	GPRASP2	FSTL4	OXSR1
CXCR3	HC	FUT7	PTTG1
DAPK2	HECW2	FXYD7	RNFT1
DENND4A	HIST2H2BE	GM10791	RPA3
DOPEY2	IL17RB	GM2A	SLC2A1
ELOVL7	KHDRBS3	GM9961	SPC25
EOMES	LIMS1	HS3ST1	SRP68
FAM26F	LRP11	IL17RE	STMN1
FAM65B	NUDT7	IL1R1	TAF9
FASL	OLFML3	IL23R	TFDP1
FCER1G	ORC1	KCNK1	THAP2
FGD5	PCSK1	LAPTM4B	TMEM199
FGL2	PDE4C	LINGO4	TXN1
FGR	PECAM1	LTA	USMG5
FILIP1L	PGAM2	LY6G6B	UXT
FOXP1	PLD1	MAF	
GAS7	PRKCA	MARK2	
GIMAP4	PRR5L	MATN2	
GIMAP8	PSTPIP2	MICAL2	
GM11435	PTPRR	MMP25	
GM156	PYROXD2	NR1D1	
GM4759	SCN8A	OLFR60	
GPR174	SESN3	PEX26	
GRAMD3	SLC29A1	PLCB4	
GVIN1	SMPDL3B	PLEKHB2	
GZMA	SP6	PLIN2	
GZMB	STARD10	PLXND1	
GZMC	TESC	PON2	
H2-AA	TIAM1	RAMP3	
HOPX	TRIM13	RARA	
HRH4	TUBA3A	RORC	
HSD11B1	ZCCHC12	SDC1	
IFITM1		SEC11C	
IFITM2		SERINC5	
IFITM3		SLC11A2	
IFNG		SLC35F2	
IL4RA		SMOX	
IRF8		SMYD1	
ITGA1		SPSB3	
ITM2A		STAB2	
KCNJ8		SUSD2	
KLRA1		TACSTD2	
KLRA3		TDRKH	
KLRA5		TICAM1	
KLRA8		TM2D3	
KLRA9		TMEM149	
KLRC1		TMEM176B	
KLRC2		TNFSF14	
KLRC3		TRPV2	
KLRD1		UCP2	
KLRG1		ZBTB7C	
KLRI1			
KLRI2			
KLRK1			
LAIR1			
LAT2			
LPAR6			
LRRC8C			
LRRK1			
LY6C1			
LY6C2			
LY9			
MAN1C1			
MAP3K8			
MBNL1			
MCOLN2			
MS4A6C			
NCALD			
NCR1			
NEURL3			
NKG7			
NR4A2			
P2RY13			
PGLYRP1			
PIK3R5			
PLEKHM3			
PPM1J			
PRF1			

NKT1	NKT2	NKT17
>NKT2 &NKT17	>NKT1 & NKT17	>NKT2 & NKT17
191	**197**	**126**
1700026L06RIK	1700040L02RIK	1300014I06RIK
1700128F08RIK	2610018G03RIK	2310007L24RIK
2700097O09RIK	2810417H13RIK	2410066E13RIK
4933440M02RIK	3830431G21RIK	3230401D17RIK
6330512M04RIK	4930452B06RIK	6720401G13RIK
A430084P05RIK	4930555I21RIK	9130401M01RIK
AB124611	4930588M13RIK	AAGAB
AHNAK	6330403K07RIK	ABI3BP
AIM1	6330406I15RIK	ACPP
AIM1L	9030617O03RIK	ADD3
ALAD	ABHD13	ADPGK
ANXA2	ABHD4	ADRB2
APOL9B	ACP5	AGPAT5
ARL4D	ADH1	ANKRD6
AW112010	ADK	APP
B4GALT1	AGFG1	AQP3
BCL2	AHCYL1	ARL5C
BIN1	AMPD1	ARNT2
BRD2	ANLN	ATG7
BTG2	ANO7	BATF
CAR2	ANP32E	BLK
CCDC136	APBB2	CACNA1A
CCL1	ARHGAP19	CCDC86
CCL4	ARHGAP20	CD37
CCL5	ARMCX1	CD72
CCR8	ASF1B	CHAD
CD160	ATP1A3	CNR2
CD2	AURKA	CORO2B
CD244	BC021785	CPE
CD63	BIRC5	CREG1
CD74	BRCA1	CRMP1
CD86	BTF3L4	CRTAM
CD97	BTLA	D17H6S56E-3
CERCAM	C330018D20RIK	DHDH
CHSY1	CASC5	DOCK5
CLDN12	CCDC126	DPY19L3
CLIC5	CCNB1	ELMOD1
CLN3	CCNG2	EMB
COMMD8	CCR9	ENTPD7
CPNE7	CCS	ERO1L
CRIM1	CD200	F2R
CSDA	CD28	FAH
CTLA2A	CD81	FAM189A1
CTLA2B	CDC45	FAM83A
CTSW	CDC6	FCHSD2
CX3CR1	CDCA5	FRMD4A
CXCR3	CENPE	FRMD6
DAPK2	CENPM	FSTL4
DENND4A	CHAF1A	FUT7
DOPEY2	CHN1	FXYD7
DSE	CHN2	GM10791
ELOVL7	CMTM4	GM2A
EOMES	CNGA1	GM9961
FAM26F	DDC	HGSNAT
FAM65B	DDX19A	HMGCL
FASL	DENND2D	HS3ST1
FCER1G	DEPDC1A	IL17RE
FGD5	DLEC1	IL1R1
FGL2	DNAHC8	IL23R
FGR	DNM3	INTS7
FILIP1L	DUSP10	KCNK1
FKBP8	DYRK4	LAPTM4B
FOXP1	E2F7	LDHD
GAS7	ENC1	LINGO4
GIMAP4	ESCO2	LMO4
GIMAP8	EXO1	LTA
GM10640	EZH2	LY6G5B
GM11435	F13A1	MAF
GM12250	F630028O10RIK	MANF
GM14005	FABP7	MARK2
GM156	FAM169B	MATN2
GM4759	FAM55B	MICAL2
GPR174	FAM55C	MMP25
GRAMD3	FAM71F2	MTSS1
GVIN1	FLRT2	MUS81
GZMA	FOXN2	NDUFS3
GZMB	FRMD7	NR1D1
GZMC	GABRR2	NUDT14
H2-AA	GATA1	OLFR60
HIGD1A	GEN1	PAOX
HOPX	GM129	PEX26
HRH4	GM14085	PFKP
HSD11B1	GM4841	PLCB4
IFITM1	GM8096	PLEKHB2
IFITM2	GM973	PLIN2
IFITM3	GNAS	PLXND1
IFNG	GPR97	PON2
IL4RA	GPRASP2	POP1
IRF8	GSN	PSD2
ITGA1	HC	PSEN2
ITM2A	HECW2	PUSL1
KBTBD2	HEY1	RAMP3
KCNJ8	HIF1A	RARA
KLF2	HIST2H2BE	RORA
KLF3	HMGN2	RORC
KLRA1	IFI27L1	SCPEP1
KLRA3	IIGP1	SDC1
KLRA5	IL17RB	SEC11C
KLRA8	IL21	SERINC5
KLRA9	IL4	SLC11A2
KLRC1	IL6RA	SLC27A6
KLRC2	KHDRBS3	SLC35C2
KLRC3	KIF23	SLC35F2
KLRD1	KLRA6	SLC41A3
KLRG1	LCK	SMOX
KLRI1	LIMS1	SMYD1
KLRI2	LRP11	SPSB3
KLRK1	LRRC49	SSR1

ILC1	ILC2	ILC3	NK cells
>ILC2 & ILC3	>ILC1 & ILC3	>ILC1 & ILC2	>ILC2 & ILC3
433	**318**	**421**	**529**
1110038D17RIK	0610010O12RIK	MARCH7	0610007P22RIK
1110054O05RIK	1110002B05RIK	SEPT5	0610037P05RIK
1700025G04RIK	1700113H08RIK	1700099P17RIK	1110038D17RIK
2210404J11RIK	1810011H11RIK	1700012B07RIK	1110054O05RIK
2810417H13RIK	2510009E07RIK	2010002N04RIK	1600012F09RIK
4632428N05RIK	2810055G20RIK	3230401D17RIK	1600014C10RIK
4930486L24RIK	3110043O21RIK	4930503L19RIK	1700020L24RIK
6030458C11RIK	4930412O13RIK	6720401G13RIK	1700025G04RIK
6330512M04RIK	4930562F07RIK	8430410A17RIK	1700040L02RIK
A430078G23RIK	4932438H23RIK	9130011J15RIK	2010012O05RIK
A430084P05RIK	9430020K01RIK	A830080D01RIK	2810006K23RIK
A530054K11RIK	A4GALT	ABCC3	2810417H13RIK
A630001G21RIK	A930011G23RIK	ABHD4	2810422O20RIK
A630089N07RIK	ABCC8	ABI3BP	3110001D03RIK
A830007P12RIK	ACBD7	ABLIM3	3110003A17RIK
AB124611	ACER2	ACPP	4430402I18RIK
ABCA1	ACOT6	ACSL1	4831426B19RIK
ACSS1	ACSBG1	ACVR2A	4930486L24RIK
ACTN1	ADAM19	ADRBK2	6330512M04RIK
ADAM4	ADCY9	AHRR	9130023H24RIK
ADAMTS10	ADM	AI848100	A430078G23RIK
ADAMTS14	AKR1C12	ALPK1	A430084P05RIK
ADAMTS8	ALDH3A1	AMICA1	A530054K11RIK
ADD3	ALOX5	AMZ2	A630001G21RIK
AFF3	ALPK3	ANXA5	A630033H20RIK
AI467606	AMPH	AP1AR	A630089N07RIK
AKR1B10	ANKS6	APOBEC1	A830007P12RIK
CD2	AURKA	APOLD1	A930038C07RIK
ANKMY2	APBB2	AQP3	AB124611
ANKRD24	AR	ARHGAP6	ABCA1
ANKRD44	AREG	ARHGAP8	ABCD1
ANXA1	ARG1	ARHGEF5	ABCG2
ANXA2	ARHGEF10L	ARPC3	ABTB2
APBB1IP	ARHGEF11	ARRB1	ACER3
ARHGAP15	ARHGEF12	ARRDC3	ACPL2
ARHGAP25	ARL5C	ARRDC4	ACSS1
ARHGEF18	ART2B	ASAH1	ACSS2
ARHGEF2	ASS1	ASPHD2	ADAMTS10
ARL2BP	ATP6V0A1	ATP1A3	ADAMTS14
ARL4C	ATP8A2	ATP8VD2	ADAP1
ARL4D	B830017H08RIK	AVIL	ADD3
ARMC7	BACE2	AW549877	AFF3
ARPC5L	BAMBI	B3GALT2	AGPAT3
ARRDC1	BCL11B	B3GALT5	AI314976
ARSB	BEX4	B4GALNT2	AI467606
ATP11B	BMP2	BC016495	AI837181
ATP1B1	BMP7	BC018473	AK3
ATP1B3	BVES	BC031181	AKR1B10
ATP6V0A2	BZW2	BCL2A1C	ALG5
ATP8B4	CACNA1D	BCL2A1D	ALKBH4
AW146020	CALCA	BMP4	ANAPC4
B3GNT5	CAR13	BTBD19	ANKRD24
B4GALT5	CCL1	BTRC	ANUBL1
BC017643	CCR4	C130039O16RIK	ANXA1
BC094916	CCR8	C4A	ANXA2
BCL9L	CD24A	C4B	APBB1IP
BID	CD6	CABLES1	APBB2
BOD1	CD81	CAP2	ARHGAP25
C030039L03RIK	CDH2	CAPG	ARHGAP30
C1GALT1	CHD7	CAV2	ARHGEF18
C630004H02RIK	CHDH	CCDC55	ARHGEF2
CAR5B	CHSY3	CCNE2	ARL4D
CASC5	CSF1	CCNG2	ARL6IP5
CASP2	CSF2	CCNI	ARPC5L
CBFA2T3	CXCL1	CCR1	ARRDC1
CCL5	CXCL2	CCR9	ARSB
CCM2	CYBB	CD164	AS3MT
CCNA2	CYP2D22	CD38	ASAP2
CCNB2	CYP2PY1	CD4	ATG4D
CCNE1	CYP51	CD83	ATG5
CCNJ	CYSLTR1	CD93	ATP11B
CCR5	D330045A20RIK	CD96	ATP1B1
CD160	DACH2	CDC42EP2	ATP1B3
CD1D1	DENND5A	CDH17	ATP6V0A2
CD1D2	DGAT2	CDH20	ATP8B4
CD2	DHCR24	CDK14	AW146020
CD22	DHX40	CHAD	B3GNT5
CD247	DIP2C	CHST12	B4GALT5
CD28	DMXL2	CKB	BAIAP3
CD3D	DOCK1	CLIC4	BC017643
CD3E	DPH5	CLNK	BC094916
CD3G	DUSP10	CNKSR3	BID
CD47	EBI3	CNN3	BLOC1S3
CD48	EEF1B2	CORO2B	C030039L03RIK
CD52	EEPD1	CPA3	C1QL3
CD55	EFNB2	CPD	CALM1
CD7	ELOVL5	CRYAA	CAPN2
CD9	ENAH	CSTAD	CAR5B
CD97	EPAS1	CTLA4	CARD6
CDC14B	EPB4.1L4A	CTSA	CBFA2T3
CDC25A	EPHA2	CTSB	CCDC88A
CDC25B	ETS2	CXCL9	CCL5
CDC42SE1	F630111L10RIK	CXCR5	CCM2
CHORDC1	FAAH	CYP2J6	CCNA2
CHPT1	FAM169B	CYP2J9	CCNB2
CHSY1	FAM183B	CYP4F16	CCNE1
CLDND2	FAM194A	D16ERTD472E	CCNJ
CLEC2I	FAM55D	DIP2A	CCR2
CLN3	FAM71F2	DHRS11	CCR5
CLOCK	FBXL21	DHRS4	CD1D1
CMAH	FBXO34	DKKL1	CD1D2
CNGA1	GALC	DLG5	CD2
CNR2	GALNT3	DMRTA1	CD247
COPA	GAS2L3	DNAH8	CD28
CRIP1	GATA3	DNAJB5	CD300LF
CRTAM	GCFC1	DNAJC12	CD47
CSPRS	GFI1	DPEP2	CD48
CST7	GFPT2	DSTN	CD52

Th1	Th2	Th17
>Th2 & Th17	>Th1 & Th17	>Th1 & Th2
1000	**1000**	**1756**
SEPT6	MARCH10	SEPT5
1110037F02RIK	0610009L18RIK	SEPT8
1110059E24RIK	1110032F04RIK	SEPT11
1700001O22RIK	1110034G24RIK	0610010F05RIK
1700025G04RIK	1110056L19RIK	1600002H07RIK
1700040L02RIK	1190005I06RIK	1600014C10RIK
2510009E07RIK	1700056E22RIK	1700008J07RIK
2610020H08RIK	1810011H11RIK	1700025G04RIK
2900026A02RIK	2310035C23RIK	1700029J07RIK
4930486L24RIK	2410015M20RIK	1700048O20RIK
4933430I17RIK	2410137M14RIK	1700128F08RIK
5430417L22RIK	2610008E11RIK	1810022K09RIK
5430427O19RIK	2700046G09RIK	1810055G02RIK
5730508B09RIK	2810408M09RIK	2010015L04RIK
5830411N06RIK	4921507P07RIK	2010204K13RIK
6330403K07RIK	4930453N24RIK	2310014L17RIK
A	4932438H23RIK	2310036O22RIK
A530064D06RIK	5830415F09RIK	2310057M21RIK
AA467197	5830416P10RIK	2410089E03RIK
AAGAB	6430571L13RIK	2700097O09RIK
ABCA3	9430020K01RIK	2810403A07RIK
ABCC3	9930012K11RIK	2900005J15RIK
ABCD1	A430078G23RIK	2900011O08RIK
ABCG1	A630033H20RIK	3000002C10RIK
ABCG2	AA987161	3110007F17RIK
ABHD4	ABCB9	3110043O21RIK
ABHD8	ABCC1	4632434I11RIK
ACADL	ABHD14B	4833439L19RIK
ACSF2	ABHD6	4930452B06RIK
ACSL4	ABTB2	4930470H14RIK
ACTN1	ACAP3	4930503L19RIK
ACVRL1	ACAT2	4930519F09RIK
ADA	ACBD7	5830418K08RIK
ADORA2A	ACCS	5830418P13RIK
ADORA3	ACOT11	6430548M08RIK
AGFG1	ACOT2	6430550D23RIK
AGFG2	ACRBP	6820431F20RIK
AGPAT5	ACSS1	8430427H17RIK
AGRN	ACSS2	9030612E09RIK
AHCY	ACTN2	9430097D03RIK
AHCYL1	ACYP1	9430015G10RIK
AHDC1	ADAM8	A430093F15RIK
AIM1L	ADAMTS10	A630001G21RIK
AIPL1	ADAMTSL4	A630089N07RIK
AKT2	ADAR	A830080D01RIK
ALAD	ADC	AA398235
ALDH5A1	ADCK1	AAAS
ALDOA	ADCY6	AATF
ALDOC	ADD3	ABAT
ANXA1	ADI1	ABCA5
ANXA2	ADK	ABCB6
ANXA6	ADPRHL2	ABCC4
AP3S1	ADRBK2	ABCC5
APAF1	AFF4	ABCC8
APBB1IP	AGER	ABCD3
APH1A	AGPAT2	ABCE1
APH1B	AHNAK	ABCF2
APOL7E	AI413582	ABHD15
APOLD1	AI462493	ABI3
APP	AI467606	ABI3BP
APPL1	AI854703	ABL2
AQP9	AK2	ACAD9
ARAP2	AKAP7	ACOT10
AREG	AKAP8	ACSL1
ARF6	AKAP8L	ACSL3
ARHGAP18	AKR1C12	ACTL6A
ARHGAP19	AKR1C13	ACTR1B
ARHGAP29	AKT1S1	ACTR3B
ARHGEF5	ALDH1B1	ACVR1
ARHGEF6	ALKBH4	ADAM12
ARID5B	ALKBH7	ADAM19
ARL5A	ALOX5AP	ADAM1A
ARL8B	ALOX8	ADAM9
ARRB1	ALS2CL	ADAMTS13
ARRDC3	AMPD3	ADAMTS6
ARSB	ANGPTL6	ADARB1
ASAH2	ANK	ADARB2
ASAP1	ANKRD23	ADCY4
ASNS	AP3D1	ADCY9
ATF6	AP4S1	ADH4
ATP11B	APOL7C	ADIPGK
ATP13A3	AQP11	AFAP1
ATP1A3	AR	AFF1
ATP1B2	ARHGAP4	AFF3
ATP2B1	ARHGEF1	AGAP1
ATP2B4	ARHGEF10	AGAP3
ATP6V1D	ARHGEF18	AHCTF1
ATP8A1	ARID4B	AHR
ATP8A2	ARL4A	AHRR
ATP8B4	ARL4C	AHSA1
AW112010	ARL6IP5	AIDA
AZIN1	ASB13	AIF1L
B2M	ASB2	AIFM1
B3GNT3	ASB6	AK1
B3GNT5	ASPSCR1	AK4
B430306N03RIK	ASS1	AKAP1
B4GALNT4	ATF3	AKAP12
BAG3	ATF5	AKAP13
BASP1	ATG16L1	AKAP2
BATF3	ATG4C	AKAP5
BBC3	ATN1	AKR1B8
BC022687	ATOX1	ALCAM
BC052040	ATP10D	ALDOART1
BC068157	ATP13A1	ALG3
BCL2L11	ATP1A1	ALG8
BCL7C	ATP1B3	ALMS1
BEND6	ATP2A3	AMACR
BHLHE40	ATP5E	AMOTL1

V1	V6	V2	V5
>V2 & V6	>V2 & V5	>V5 & V6	>V2 & V6
23	**387**	**194**	**408**
C1QL3	ACSL3	ACVR2A	ACSF2
CCL5	ADAMTS3	ADAM12	ADH1
CD8B1	ADAMTS6	ADAM8	ADRB1
CRTAM	ADAMTSL3	ADRB2	AHRR
DAPL1	ADK	AHCYL2	ALPI
EOMES	AKAP6	AI504432	ANXA4
GPR15	AKR1C12	AI646023	AOAH
GRIA3	AKR1C18	ANKRD35	APH1B
HMCN1	ALS2	ANKRD6	APLP1
IFT80	ALS2CL	AOP3	APLP2
ITGA4	ANP32E	ARHGAP21	APOA1
KIT	APOO	ARHGAP26	APOA4
KLRI1	APOOL	ARHGAP31	APOL10B
MIR365-1	ARHGAP11A	ARID5A	APOL9A
MS4A4C	ARHGAP24	ARNTL	APOL9B
PRR5L	ARL4D	ATF6	APPL2
RRAS2	ASAP1	ATOH8	ARAP3
SELL	ASF1B	ATP10D	ARHGEF5
THEMIS	ASPM	ATP2B1	ARID3A
TNFSF8	ATIC	B3GNT5	ARRDC3
TRIO	ATP1B1	BIK	ARRDC4
TSGA10	BC021614	BLK	ART2B
TUBA3B	BC094916	C630004H02RIK	AS3MT
	BRIP1	CAMK2D	ASB2
	BTLA	CCDC109B	ASPH
	BUB1	CCR2	ATG4C
	BUB1B	CCR6	ATP6V0A2
	BZW2	CCR6L1	AUH
	C330027C09RIK	CD44	B3GALT5
	CACNA1D	CD55	B3GNT7
	CAP2	CDC14B	B4GALNT2
	CASC5	CDH10	B4GALNT4
	CASD1	CDON	BAIAP3
	CBX5	CLIP1	BC005624
	CCDC125	CLOCK	BC013712
	CCNA2	CORO2B	BC016495
	CCNB1	CPEB2	BCL2
	CCNB2	CPM	BCL2L11
	CCNE2	CRY1	BEND7
	CCR10	CRYBG3	BMF
	CCR4	CXCR6	BMP2K
	CCR8	CYP2S1	C030046I01RIK
	CD28	CYSLTR1	C1QTNF6
	CD4	DERL3	CABLES1
	CD40LG	DKKL1	CAMK2N1
	CD5	DUSP7	CAPN3
	CD6	EDARADD	CAR2
	CD81	ELL2	CASZ1
	CD9	EMB	CCDC104
	CDC6	EMP3	CCDC134
	CDCA5	EPAS1	CCDC136
	CDCA7	ERO1L	CCDC80
	CDK1	ESYT2	CCL3
	CDKN2C	ETV6	CCL4
	CENPE	F2RL2	CCL5
	CENPH	FAM117A	CCNI
	CENPK	FAM124B	CCNO
	CEP55	FAM169B	CCRL2
	CES2D-PS	FAM65B	CD101
	CHDH	FCHO2	CD200R1
	CHEK1	FLOT1	CD200R2
	CHST15	FOSB	CD200R4
	CHST2	FSTL4	CD244
	CKS1B	GAB3	CD38
	CKS2	GABBR1	CD3E
	CMTM7	GALM	CD7
	CNTNAP1	GGT1	CD72
	CPNE7	GLIPR2	CD8A
	CSF1	GLT25D2	CD96
	CTLA2A	GM2A	CDH1
	CX3CR1	GM527	CDYL2
	CXXC5	GOLM1	CELA1
	CYCS	GPR132	CHST12
	D030056L22RIK	GPR183	CHSY1
	DEPDC1A	GPR44	CLDND2
	DFNA5	GPRIN3	CLIP2
	DLGAP5	H60B	CLNK
	DNA2	HBB-B1	CLSTN1
	DNAHC8	HBB-B2	CNIH2
	DPP4	HLF	CNNM2
	DSTN	HNRPLL	CCNZ2
	DTL	IFI203	CREB3L1
	DUSP2	IFNGR1	CRTAM
	DUT	IGF1R	CTLA4
	EIF3M	IL17F	CTNNBIP1
	ENG	IL17RA	CYP2J6
	EPHA3	IL17RC	CYP2J9
	ERH	IL17RE	CYP51
	ESCO2	IL1R1	CYTH3
	ETV5	IL23R	D8ERTD82E
	EXO1	IL2RA	DAPK2
	EZH2	IL7R	DCBLD2
	F630043A04RIK	IRAK3	DDC
	FABP7	ITGA5	DDX28
	FAIM	ITGB5	DENND4A
	FAM20A	KBTBD11	DHCR24
	FAM49A	KCNA3	DHCR7
	FAM54A	KCNK1	DISP1
	FAM60A	KLF2	DOK1
	FAM81A	KLF3	DSP
	FBXO5	LAPTM4B	DTX1
	FCRL1	LINGO4	DUSP10
	FGF2	LONRF3	DUSP5
	FHL2	LPCAT2	DUSP6
	FIGNL1	LRRC25	EEF2K
	FLRT2	LRRC8B	EFCAB4B
	FOLR4	LRRN4	EFHD2
	FZD6	LTB4R1	EHD1

PTPN4
QRFP
RECK
RGS1
RGS18
RNF13
SAMD3
SEPN1
SERPINA3H
SERPINB9
SERPINB9B
SERPINI1
SIDT1
SLAMF7
SNX10
SPIN2
SRC
STYK1
SYTL2
SYTL3
TACC1
TBX21
TMEM2
TMEM37
TNFSF8
TSC22D3
TSPAN4
TXNIP
TYROBP
WIPF1
XCL1
ZCCHC18

LAIR1
LAT2
LITAF
LPAR6
LRRC8C
LRRK1
LY6C1
LY6C2
LY6I
LYZ1
LYZ2
MAGOHB
MAN1C1
MAP3K8
MBNL1
MCOLN2
MS4A6C
NCALD
NCR1
NEDD4
NEURL3
NKG7
NR4A2
OASL1
P2RY13
PANK3
PDE7A
PEA15A
PGLYRP1
PIK3R5
PITPNC1
PLEKHM3
POGK
PPM1J
PRF1
PTPN4
PTPN6
QRFP
RCBTB2
RECK
RGS1
RGS18
RNF13
SAMD3
SEPN1
SERPINA3H
SERPINB9
SERPINB9B
SERPINI1
SIDT1
SLAMF7
SLC2A3
SMAP2
SNX10
SPAG9
SPIN2
SRC
ST3GAL4
STYK1
SYTL2
SYTL3
TACC1
TAPBPL
TBX21
TGFBR2
TMEM2
TMEM37
TNFRSF18
TNFSF8
TPM1
TPM4
TSC22D3
TSPAN4
TXNIP
TYROBP
UBLCP1
UIMC1
WHSC1L1
WIPF1
XCL1
ZCCHC18
ZFP36L2
ZYX

LXN
LYPD6B
LZTFL1
MAGED2
MAPK11
MBOAT1
MCM10
MGST2
MTX2
NAA20
NBR1
NCAPG2
NCAPH
NRP2
NTRK3
NUDT7
NUP153
OLFML3
ORC1
PABPC1
PCSK1
PDE4C
PDE7B
PECAM1
PGAM2
PGCP
PGK1
PHGDH
PLAC8
PLAUR
PLD1
PPIC
PRDX2
PRG4
PRKCA
PRR5L
PSTPIP2
PTGIR
PTPLAD1
PTPN5
PTPRR
PXMP3
PYROXD2
RCAN3
RCBTB1
RGS12
RPRM
RRM2
SAMHD1
SCD1
SCD2
SCN8A
SDHB
SEC63
SESN3
SETX
SGK3
SGOL1
SLC22A3
SLC29A1
SMC2
SMPDL3B
SNX10
SOX4
SP6
SPNB2
ST13
ST8SIA6
STARD10
STMN1
TCF25
TCF7
TESC
THEMIS
TIAM1
TNFRSF4
TOP2A
TPMT
TRIM13
TRP53BP1
TSPAN32
TTC3
TUBA3A
TUBB5
TWSG1
TYMS
USP38
XKR8
ZCCHC12

STAB2
SUSD2
TACSTD2
TCEAL3
TCEB3
TDRKH
TICAM1
TM2D3
TMEM149
TMEM176B
TNFSF14
TNS4
TRPV2
TUBE1
UCP2
UTP11L
ZBTB7C
ZFP459

CTSD
CYB5B
CYM
D10WSU102E
D14ABB1E
D1ERTD622E
D330012F22RIK
D4WSU53E
D8ERTD82E
D930015E06RIK
DAPL1
DDX39
DDX43
DEF6
DENND2D
DGKA
DGKZ
DIDO1
DNAHC8
DOCK11
DOCK9
DPH2
DPY19L1
DSCAM
DTX3L
EFCAB4B
EFHC2
EFHD2
EHD3
ELOVL7
ELTD1
ENPP1
ENTPD4
EOMES
EPSTI1
ESYT1
EYA1
F2RL1
FAM120B
FAM33A
FAM53B
FAM65B
FAM78A
FAM78B
FBXL2
FBXO22
FCGR2B
FCHSD2
FGF13
FGR
FLNA
G3BP2
GAS7
GBP5
GDF11
GIMAP8
GM11435
GNPNAT1
GNPTAB
GOLGA1
GOLM1
GOLPH3L
GPR137B
GPR15
GPR155
GPR174
GPR18
GPR21
GPR68
GPRIN3
GRAMD3
GRAMD4
GSG2
GTDC1
GVIN1
GZMA
GZMM
H2-Q6
H2-T24
H6PD
HAAO
HERC3
HIST1H2AK
HIST1H2BN
HN1
HOPX
HS3ST3B1
HSD11B1
I830012O16RIK
IFI44
IFI47
IFIT2
IFNAR2
IKZF1
IL10RB
IL16
IL17RA
IL18RAP
IL20RA
IL21R
IRGM1
ITGA2
ITGAM
ITGAX
ITGB1
ITGB1BP1
ITGB2
ITM2A
JAK1
KBTBD4
KCNAB2
KCNIP3
KCNJ8
KIFC3

GLB1
GLRX
GM7257
GM889
GRIN2D
H2-OA
HAVCR2
HBA-A1
HBA-A2
HDAC5
HDC
HDX
HES1
HGF
HIST1H2BC
HIST1H2BE
HIST1H2BG
HIST2H2BB
HLF
HMCN1
HOMER2
HPGDS
HPN
HS3ST1
HSPB11
HTR1B
IFNGR2
IGFBPL1
IL13
IL17RB
IL1RL1
IL4
IL5
IL6
IL9R
INPP4B
IPMK
IRF4
ITK
JDP2
KCNA4
KCNN4
KCNQ5
KIF23
KLF5
KLK8
KLRG1
KRT80
LGALS7
LGMN
LMO4
LPCAT2
LPHN2
LRRC34
LRRC52
LY6A
LY6C1
LY6C2
MAP4K3
MBOAT1
MC5R
MED12L
MICAL3
MNS1
MRAS
MUC1
MXI1
MYO1D
NAIP1
NAIP5
NAIP6
NAV2
NCKAP5
NEB
NEO1
NFIX
NFKB1
NHS
NMUR1
NPNT
NUCB2
OLFR1009
OLFR1037
OLFR1134
OLFR1168
OLFR1173
OLFR1226
OLFR1245
OLFR1372-PS1
OLFR1384
OLFR340
OLFR478
OLFR706
OLFR714
OTX1
P4HA2
PAPSS2
PARD3
PCSK1
PDCD1
PDCD1LG2
PDE4D
PDE7B
PENK
PGCP
PKIA
PLAUR
PLCL1
PLSCR2
PLXDC1
POPDC3
POU2F2
PPARG
PPM1L

DUS2L
DUSP4
E2F3
EGFL6
EIF2C4
EMD
EMP1
ENTPD1
EPB4.1L5
EPS8
EPS8L3
ETV5
F2R
F2RL2
FAH
FAM134B
FAM184B
FAM20A
FAM46C
FAM82A1
FAM98B
FBXL17
FFAR2
FGF16
FHL2
FNBP1L
FRYL
GABARAPL1
GATAD1
GCNT2
GDA
GJB2
GLT25D2
GM11818
GM166
GM5635
GNA13
GNG12
GNG2
GNG5
GOLIM4
GPNMB
GPR146
GPR157
GPR183
GPR34
GPR97
GRAMD1B
GRB7
GSTM4
GSTM5
GSTT2
GZMB
GZMC
GZMD
GZME
H1F0
HBP1
HERPUD1
HK2
HMGB3
HOXA5
HOXA6
HPSE
HS6ST2
HSD17B11
HSPA13
HTRA1
ICOS
IER5L
IFI30
IFNGR1
IGFBP4
IGFBP7
IL17RE
IL1R1
IL1R2
IL1RL2
IL22
IL23R
ING3
ING5
INPP4A
INTS12
IRAK3
IRF5
IRF8
ISCU
ITGB3BP
ITGB5
JMJD1C
KCNK1
KRT4
L1CAM
LANCL2
LARGE
LGALS3
LIN7C
LINGO4
LITAF
LRRC49
LRRC8B
LRRK2
LTA
LY6G5B
LY86
LYSMD2
LYSMD3
MAF
MAFF
MAPK10
MARCKSL1
MARVELD1
MBD2

CD55
CD68
CD7
CD9
CD97
CDAN1
CDC14B
CDC25B
CDC34
CDC42SE1
CDCA7L
CDH22
CDK2AP1
CDKN2C
CDKN2D
CGGBP1
CHPT1
CHRNE
CHSY1
CLDND2
CLEC2D
CLEC2I
CLEC4E
CLIP3
CLOCK
CMA1
CMKLR1
CRIP1
CRTAM
CSDA
CSPRS
CST7
CSTF2T
CTLA2A
CTSC
CTSD
CUEDC1
CX3CR1
CYM
CYP17A1
D1ERTD622E
D330012F22RIK
D4WSU53E
D8ERTD82E
D930015E06RIK
DAPK2
DCXR
DDX39
DGKH
DGKZ
DNAHC8
DNAJC15
DOCK11
DOK2
DPH2
DPY19L1
DUSP2
DUSP22
EFCAB4B
EFHD2
EHD3
EIF5A2
ELOVL7
ELTD1
ENPP1
ENTPD1
EOMES
EPSTI1
ESD
ESYT1
EYA1
F2RL1
FAM105B
FAM26F
FAM53B
FAM65B
FAM69A
FBXL2
FCGR2B
FCRL6
FLNA
FRY
GALNT6
GAS7
GEMIN7
GGCT
GIMAP1
GM11435
GNPNAT1
GNPTAB
GOLM1
GOLPH3L
GPC1
GPR137B
GPR160
GPR174
GPR25
GPRIN3
GPX8
GRAMD3
GRAMD4
GSG2
GSTM1
GTDC1
GVIN1
GZMA
GZMB
GZMK
GZMM
H2AFZ
HAAO
HERC3
HEXB

BMF
BMP2K
BNIP3
BRDT
BRE
BSPRY
BST1
BTBD1
BTG1
BTLA
C1QTNF1
C1QTNF6
C330007P06RIK
CAB39
CABLES1
CACNB3
CACNB4
CAGE1
CAPN2
CAR11
CARD11
CASP1
CASP3
CASP4
CASS4
CAV2
CBLB
CBX3
CCDC102A
CCDC136
CCDC92
CCL5
CCND3
CCNI
CCR5
CCRL2
CD163L1
CD164
CD200R1
CD200R4
CD28
CD38
CD8A
CD9
CD93
CDC14A
CDK14
CDK19
CDKN2A
CDKN2C
CDKN3
CDNF
CDS2
CELF2
CELSR1
CENPA
CENPM
CEP170
CHD7
CHPT1
CHST11
CHST15
CHST2
CHSY1
CKB
CLEC12A
CLEC2I
CLIC1
CLIC4
CLIP2
CLNK
CLSTN3
CMAH
CMAS
CNRIP1
COBLL1
COPS2
COPS4
CORO2A
COX5A
CPM
CPNE3
CS
CSF1
CSF2
CSRP2
CTDSP2
CTLA2A
CTSB
CUTA
CXCR1
CXCR2
CXCR3
CXCR6
CYB5R4
CYP4F39
CYP51
CYSLTR2
CYTH3
CYTIP
D16ERTD472E
D8ERTD82E
D930015E06RIK
DAP
DAPK2
DCUN1D3
DDAH2
DDX60
DENND4A
DENND4C
DEPDC1B
DES
DGAT1
DGKH

ATP6V0B
ATP6V0E
AUH
AVIL
BAIAP2
BATF
BBS9
BC021614
BC037034
BCAM
BCKDHB
BCL11B
BET1L
BHLHE41
BID
BIN1
BMP7
BOLA2
BRAP
BRI3
BSCL2
BTC
BTG2
C030006K11RIK
CACNA1C
CACNB1
CALCRL
CAMK1D
CAMK2B
CAMKK2N1
CAMTA2
CARD6
CARHSP1
CATSPERB
CBR1
CBX4
CBX7
CCDC101
CCDC115
CCDC22
CCDC32
CCDC88B
CCDC9
CCIN
CCM2
CCNO
CCR1
CCR8
CD1D1
CD3D
CD79B
CD82
CD83
CD96
CDC42BPG
CDC42SE2
CDH1
CHN2
CHPF2
CHST10
CHURC1
CIB2
CISD2
CISH
CITED2
CKLF
CLCF1
CLCN3
CLCN4-2
CLCN5
CLEC2D
CLN3
CLN5
CMPK2
CMTM3
CMTM8
CNGA1
CNIH4
CNP
CNR2
CNST
CNTROB
COL11A2
COL1A1
COL23A1
COMMD2
COMMD6
COMMD7
CORO7
COX11
COX16
CR1L
CREG1
CRIP1
CRLF2
CRTC1
CSK
CST6
CST7
CTAGE5
CTSE
CTSF
CTTN
CXCR4
CXCL16
CYB561D2

AMPH
ANAPC13
ANGPTL2
ANKLE1
ANKRD13B
ANKRD17
ANKRD26
ANKRD37
ANKRD50
ANKRD52
ANP32A
AOAH
AP1AR
APEX2
APITD1
APLF
APLP2
APOL9B
APOO
AQP3
ARGLU1
ARHGAP12
ARHGAP21
ARHGAP27
ARHGAP31
ARHGAP32
ARHGAP33
ARHGAP39
ARHGAP5
ARHGDIG
ARHGEF19
ARHGEF9
ARMC9
ARMCX2
ARMCX4
ARMCX6
ARNTL
ART2A-PS
ASB14
ASH2L
ASPH
ASXL1
ATAD2
ATAD3A
ATAD5
ATAT1
ATP1A2
ATP1B1
ATP2A2
ATP6V0A1
ATP6V0D2
ATP6V1G2
ATP7B
ATPIF1
ATR
ATRN
ATRNL1
ATXN10
ATXN2
AVPI1
AXL
B230319C09RIK
B3GALNT2
B3GNT8
BC018473
BC030476
BC030867
BC068281
BCAR1
BCAT1
BCL2A1B
BCL2A1C
BCL2A1D
BCL2L2
BDP1
BEGAIN
BEND3
BEND4
BHLHB9
BIRC3
BLCAP
BMP1
BMPR2
BPTF
BRCA2
BRD3
BRD7
BRIX1
BRMS1L
BRPF3
BUD31
BZW2
C1QBP
C1S
C330024D21RIK
C330027C09RIK
CACNB2
CACYBP
CALHM2
CAMKK2
CAMSAP1
CAPG
CAPN11
CAPRIN2
CAPSL
CAR12
CAR13

GADL1
GAS5
GEMIN6
GEN1
GM12238
GM4759
GM885
GMNN
GNPNAT1
GPNMB
GPR155
GPR174
GTF2IRD1
GYPC
H19
H1F0
HC
HDC
HDDC2
HELLS
HEY1
HHEX
HIBCH
HIF1A
HIST1H1A
HIST1H2AB
HIST1H2BB
HIST1H2BF
HIST1H2BG
HIST1H2BJ
HIST1H2BK
HIST1H2BL
HIST1H2BN
HIST1H4A
HIST1H4B
HIST1H4C
HIST1H4D
HIST1H4F
HIST1H4K
HIST1H4M
HIST2H2BB
HIST4H4
HIVEP3
HMGA2
HMGB3
HMMR
HRH4
HSPD1
I830012O16RIK
ID3
IFI27L1
IFI27L2A
IFI30
IFI44
IFIT1
IFIT2
IFIT3
IGF2BP3
IGFBP4
IIGP1
IL13
IL17RB
IL21
IL4
IL6RA
INPP4B
IPCEF1
ITGA4
JUB
JUP
KCNN2
KIF11
KIF15
KIF20A
KIF2C
KIF4
KLF12
KLRA1
KLRA10
KLRA3
KLRA6
KLRA9
KLRB1B
KLRB1C
KLRC1
KLRC2
KLRC3
KLRI2
KNTC1
KPNA2
LCLAT1
LEF1
LGI2
LPCAT4
LRRC8
LRRTM1
MAGOH
MARCKSL1
MBOAT1
MCM5
MCM7
MGST2
MIR181A-1
MIR181B-1
MKI67
MPP6
MPP7
MRPS6
MSRA
MTX2
MX2
MYB
NANOS1
NCAPG

LY6A
LY6G5B
MATN2
MGAT5
MIF4GD
MIR202
MIR344
MMP14
MMP25
MTSS1
NAV2
NPL
NR1D1
NR1D2
ODC1
OLFR525
OLFR527
P2RY1
PCSK1
PDE5A
PI4K2A
PISD-PS1
PLIN3
PLP2
PLXDC2
PLXNA1
PLXND1
PRELID2
PROS1
PRSS12
RAMP3
RAPGEF4
RARG
RASA3
RASA4
RASGRP2
RASSF3
RBPMS2
RET
RORC
S100A4
S100A6
S1PR1
SAMHD1
SCPEP1
SDC1
SELL
SEMA4B
SEMA4F
SEPP1
SERPINB1A
SGK1
SH3BGRL2
SH3PXD2B
SLAMF1
SLC27A6
SLC35F2
SLC9A2
SMOX
SOCS3
SOX13
SPOCK2
SSH2
ST3GAL6
TDRKH
TMEM176A
TMEM176B
TMEM65
TNFRSF25
TNFRSF26
TSC22D1
TSPAN31
TUBA8
ZDHHC2
ZFP462
ZFP516
ZNRF1

ELMO2
ENPP5
ENTPD1
EPB4.1
EPCAM
ERRFI1
EXOC3
FABP2
FADS1
FADS2
FAM109B
FAM135B
FAM46C
FASL
FCER1G
FCGR3
FDFT1
FDPS
FES
FGL2
FGR
FOSL2
FOXO3
FRMD4B
FRMD5
GABARAPL1
GALNS
GBP5
GCA
GCET2
GCNT1
GCNT2
GFI1
GGTA1
GIMAP3
GIMAP6
GIMAP7
GKAP1
GLCCI1
GLP1R
GM11435
GM12253
GM156
GM4956
GNAS
GNB5
GNGT2
GOLIM4
GP49A
GPD2
GPR18
GPR34
GPR55
GPR56
GPX8
GRB7
GZMA
GZMB
GZMK
HECTD2
HEYL
HIC1
HIP1
HMGCR
HMGCS1
HPGDS
HSD17B7
HSPA2
HVCN1
IDH1
IDI1
IER5L
IGF2R
IGSF5
IL12RB2
IL21R
IL2RB
IL34
IL6ST
INPP4A
INSIG1
INTU
IRF8
ITGA1
ITGAD
ITGAE
ITGAM
ITGAX
ITIH5
JDP2
JUNB
KCNG3
KIT
KLHL4
KLRB1A
KLRD1
KLRI1
KY
LAG3
LASS6
LAT2
LDLR
LGALS2
LILRB4
LIMK1
LITAF
LPIN2
LRRC8C
LRRC9
LRRK1
LSS
LTA4H
LYN
MAP4K1

KLF12
KLHL20
KLHL4
KLHL6
KLRA1
KLRA10
KLRA3
KLRA5
KLRA6
KLRA8
KLRA9
KLRB1A
KLRB1C
KLRC1
KLRC2
KLRC3
KLRD1
KLRE1
KLRI1
KLRI2
KLRK1
LAT2
LAX1
LCN4
LDLRAP1
LEF1
LFNG
LGALS1
LIMD2
LIMS1
LPAR5
LRMP
LRRK1
LY6C1
LY6C2
LYST
MFSD8
MKI67
MS4A4B
MS4A4C
MS4A6B
MS4A6C
MTERF
MTIF3
MYB
MYO1F
NBEAL2
NCK1
NEBL
NOD1
OAS1A
OAS1B
OGT
ORAI2
ORMDL1
OSBPL5
OXSM
PAM
PARP11
PDE2A
PDGFB
PGLYRP1
PHF11
PIK3R5
PILRB1
PION
PJA2
PLEK
PLEKHA5
PLXNC1
POGK
POLE2
POT1A
POT1B
PPARGC1A
PQLC3
PRF1
PRKCB
PRKCQ
PRR5L
PTCD2
PTPN12
PTPN4
PTPRC
PYCARD
PYHIN1
QRFP
RAB7L1
RACGAP1
RANBP10
RAP1A
RAP2B
RAPH1
RARG
RASA1
RASA3
RASGRP2
RELT
RFX3
RGS3
RHOQ
RNF144A
RNF219
RRAGB
RRAS2
RRM2
RSL1
RTP4
RTTN
S100A6
S1PR1
S1PR4
S1PR5
SAMD3
PPP2R3A
PRNP
PSMC5
PTGIR
PTK2
PTP4A1
PTPN13
PTPN9
RAB11FIP5
RAB27B
RAB30
RAB4A
RAD51L1
RASGRP4
RBM47
REM2
RET
RETNLB
RGS12
RIPK4
RNF128
RPL11
RPL19
RPL22
RPL24
RPL26
RPL27
RPL27A
RPL30
RPL31
RPL35
RPL35A
RPL36
RPL36A
RPL37A
RPLP1
RPRL2
RPS13
RPS17
RPS21
RPS24
RPS27A
RPS28
RPS3
RPS8
RPS9
RPSA
RRP15
RUNX1T1
RXRG
SCAMP1
SCEL
SEMA3E
SERPINE1
SLAIN1
SLC18A2
SLC6A12
SLC7A5
SLC7A8
SOAT1
SOCS5
SPCS3
SPNS3
SPRY1
SSXB10
ST6GALNAC5
STAB2
STXBP6
SV2B
SYNE1
TANC2
TCP11L1
TGM2
THSD4
TKTL1
TLE1
TLR1
TMEM146
TMEM164
TNFRSF10B
TNFSF18
TPH1
TSPAN13
UBAS2
UBB
UBC
UBE2E2
UBE2L6
UNC5B
VIPR2
VMN1R179
VMN1R6
YPEL2
ZC3H12C
ZDBF2
ZFP92
MDFIC
METTL4
MGAT4A
MICAL2
MINA
MMP23
MPZL3
MSRA
MTAP7D3
MYO5A
NCOA7
NDRG1
NEDD9
NEIL1
NFAM1
NFE2L2
NIF3L1
NLRP1B
NMBR
NOX1
NPAS2
NR1D1
NRGN
NT5E
OASL2
OAT
OCRL
OGFRL1
OLFR1342
OLFR46
OLFR60
OPTN
ORAI1
OSGIN2
P2RX7
PARP1
PARP12
PDE4B
PDE5A
PDP1
PDZD2
PEX13
PGM1
PGM2L1
PHYH
PIK3C2B
PIK3R1
PLCB4
PLCXD2
PLEKHG1
PLEKHM3
PLK3
PLK4
PLTP
PODNL1
POP4
PPP1R11
PPP1R2
PPP1R3B
PRAM1
PRC1
PRELID2
PRR5
PRRG1
PRRG4
PSAP
PSD2
PTGES
PTMS
PTPN3
PTPRA
PTPRM
RAB7
RABGEF1
RAI14
RASA2
RASGEF1B
RASGRP3
RASL11A
RBBP8
RBM11
RBM24
RBPMS2
RCBTB2
RFK
RGNEF
RGS9
RHOBTB1
RHOC
RHOD
RIN2
RIPK2
RNF24
RNFT1
RORC
RPN1
RPS7
RSU1
RYBP
RYK
S100A1
S1PR3
SAP30
SAT1
SCPEP1
SCRT1
SDC1
SDC2
SEC24D
SELM
SEMA4F
SEPP1
SERINC2
SERPINB1A
HGSNAT
HHEX
HIST1H1B
HIST1H2AF
HIST1H2AK
HIST1H2AN
HIST1H2BB
HIST1H2BC
HIST1H2BL
HIST1H3G
HN1
HSD11B1
HYLS1
I830012O16RIK
IFI47
IFIT2
IL10RA
IL10RB
IL16
IL17RA
IL18RAP
IRGM1
ITGA2
ITGA6
ITGAD
ITGAM
ITGAX
ITGB1
ITGB1BP1
ITGB2
ITM2A
JAK1
KBTBD4
KCNAB2
KCNIP3
KCNJ8
KCTD1
KHDC1A
KHDC1B
KLF12
KLF2
KLHL20
KLHL30
KLHL4
KLHL6
KLRA1
KLRA10
KLRA3
KLRA5
KLRA6
KLRA8
KLRA9
KLRB1A
KLRB1C
KLRC1
KLRC2
KLRC3
KLRD1
KLRE1
KLRI2
KLRK1
KPNA2
KTI12
LACTB2
LAIR1
LASS2
LAT2
LAX1
LDLRAP1
LFNG
LGALS1
LIMS1
LPIN1
LRMP
LRRK1
LY6C1
LY6C2
LYRM2
LZTS1
MAG
MCAM
MED30
MED8
MEF2C
METTL5
MOCS2
MORC3
MS4A4B
MS4A4C
MS4A6C
MTERF
MTIF3
MYB
MYLIP
NAGK
NBEAL2
NCALD
NCK1
NHP2L1
NIP7
NKG7
NOD1
NPC1
NRARP
NT5C
OAS1B
ORAI2
ORMDL1
OSBPL5
PAM
PDCD10
PDE2A
PDGFB
PEX5L
DHCR7
DHX58
DISP1
DKKL1
DLG3
DNAJB13
DNAJC15
DNM1
DOCK9
DOK1
DPY19L1
DPYSL2
DSE
DSG2
DYNLRB2
DYRK2
DZIP1
E330009J07RIK
ECE1
EDEM1
EEFSEC
EFCAB10
EFHD2
EFNA1
EFR3A
EHD1
EID1
EIF2AK2
EIF4E3
ELOVL5
ELOVL6
EMB
EMILIN2
ENPP1
ENPP4
ENPP5
EPHX4
EPS8
EPSTI1
ERAP1
ERI2
ERMN
ERMP1
ERO1LB
ERRFI1
ESPN
ESPNL
ESR1
ETV3
ETV5
EXOC6
EZR
F2RL1
FADS2
FAH
FAM102B
FAM107B
FAM110A
FAM114A1
FAM122B
FAM132A
FAM168A
FAM20A
FAM26F
FAM49A
FAM63B
FAM64A
FASL
FBLN1
FBXL5
FBXO28
FCER1G
FCHO2
FDPS
FFAR2
FGGY
FGL2
FHL2
FILIP1
FKBP5
FNDC3A
FNTB
FOXJ1
FRMD4B
FURIN
FUT4
FUT8
FXYD1
FXYD5
FXYD7
FYN
FZD5
GAB3
GADD45G
GALE
GALNS
GALNT3
GALNT7
GAPDH
GAS2L3
GAS7
GATAD1
GATSL2
GBE1
GBP2
GBP3
GBP4
GBP6
GCA
GCAT
GDF11
GFPT1
GGTA1
CYBRD1
DHX16
CYP4F16
CYP4V3
CYSLTR1
D630039A03RIK
DAND5
DAPK1
DAPK3
DBNDD2
DCAF4
DCLK2
DDC
DDIT3
DDX26B
DEDD2
DENND1A
DENND1C
DENND3
DFFB
DGKA
DHRS11
DHRS3
DHRSX
DMD
DNAJB9
DNASE1L2
DNASE2A
DOCK2
DOK2
DPP7
DTWD2
DTX4
DUSP1
DUSP10
DUSP2
DUSP23
DUSP6
E130311K13RIK
E4F1
EAR2
ECM1
EFNA5
EHHADH
EIF5
ELF1
ELF2
EMG1
EMILIN1
EML1
EML3
EMP3
ENGASE
ENTHD1
ENTPD1
ENTPD6
EOMES
EPAS1
EPB41L1
EPCAM
EPHA2
EPHX1
ERN1
ESCO1
ESRRA
EYA2
F2RL3
FAAH
FADD
FAM101B
FAM105A
FAM117A
FAM117B
FAM120A
FAM129C
FAM160B2
FAM19A3
FAM20B
FAM46A
FAM63A
FAM65C
FAM83H
FAU
FBRS
FBRSL1
FBXO17
FBXO27
FBXO31
FBXO33
FBXO4
FCGRT
FCHSD2
FCRLS
FGFR1
FILIP1L
FLAD1
FLCN
FLT3L
FN3K
FNDC3B
FRAT1
FRAT2
FRMPD1
FRY
FTL1
FUT11
FYB
FZD10
GABARAPL2
GABRB3
GAL3ST1
GALNT10
GATA1
GATA3
CAR5B
CARM1
CASK
CASKIN2
CASP7
CAZ1
CBX2
CCAR1
CCBL2
CCDC112
CCDC116
CCDC122
CCDC132
CCDC137
CCDC157
CCDC30
CCDC34
CCDC57
CCDC58
CCDC63
CCDC74A
CCDC88A
CCL3
CCL4
CCNE1
CCNE2
CCNYL1
CCR3
CCRN4L
CCT3
CCT6A
CCT8
CD101
CD109
CD200
CD209C
CD24A
CD300A
CD33
CD3EAP
CD40
CD5
CD5L
CD74
CDC123
CDC14B
CDC25A
CDC42BPA
CDC42BPB
CDC42EP4
CDC45
CDC6
CDC7
CDCA7
CDH23
CDK16
CDK2
CDK2AP1
CDK5
CDK6
CDK8
CDKL3
CDKL5
CDKN1A
CDR2
CDR2L
CDV3
CDYL
CELA1
CELF1
CELSR2
CENPH
CENPI
CENPT
CEP110
CEP135
CEP152
CEP170
CEP250
CEP290
CEP350
CEP57
CEP78
CERK
CERKL
CFDP1
CHAF1A
CHCHD4
CHD1
CHD9
CHEK1
CINP
CIRH1A
CKS2
CLASP1
CLEC2L
CLGN
CLSPN
CLUAP1
CMKLR1
CNDP2
CNIH3
CNKSR3
CNNM4
CNOT10
CNTLN
COL15A1
COL5A1
COLEC12
COPS5
COPS7B
COQ3
COQ7
COX6C
NCAPG2
NCAPH
NCR1
NDUFB6
NDUFC2
NEIL3
NEK2
NET02
NIPAL1
NME1
NOP10
NPAS4
NPM3
NPM3-PS1
NRGN
NRP1
NSG2
NTRK3
NUDCD2
NUF2
OAS2
OASL2
OLFR161
ORC6
PACSIN1
PAK1
PARD6G
PBK
PDCD1
PDCD1LG2
PGCP
PHGDH
PITPNM2
PLA2G7
PLAC8
PLEKHO1
PLK1
PLK2
PLXNA3
POLE
POMP
PPA1
PPIC
PPIL1
PRC1
PRDX1
PRG4
PRIM1
PSAT1
PSMB6
PSMG1
PSMG2
PTPN13
PXMP3
RAD54L
RALYL
RAP1A
RAP2C
RAPH1
RASA1
RBPMS
RCBTB1
RILPL2
RIN2
RNF2
RNU12
RNU73B
ROCK2
RPL23A
RPS12
RPS17
RPS27L
RRM2
SAMD3
SCCPDH
SGK3
SH2D1A
SHCBP1
SHMT1
SLAMF6
SLC12A2
SLC14A1
SLC15A1
SLC16A1
SLC22A3
SLC25A13
SLC25A17
SLC25A5
SLC29A1
SLC44A1
SLC5A3
SLC7A5
SLC9A7
SLFN1
SLFN3
SMC2
SMTN
SNHG1
SNORA16A
SNORA23
SNORA34
SNORA44
SNORA65
SNORA69
SNORA74A
SNORD104
SNORD118
SNORD15A
SNORD15B
SNORD16A
SNORD1C
SNORD22
SNORD35A
SNORD38A
MAPK3
MAPRE2
MAX
MBD2
MCAM
MCART6
MCOLN3
MCTP2
METRNL
MLKL
MLLT4
MRAS
MRGPRA9
MTA3
MYO1E
MYO6
NAAA
NAIP5
NAIP6
NAPSA
NCALD
NCF1
NEDD4L
NEDD9
NEURL3
NFIL3
NKG7
NLRP1B
NMB
NOD1
NR4A1
NR4A2
NR4A3
NRCAM
NSDHL
NTAN1
NUMBL
OPTN
OS9
OSGIN1
OSTF1
P2RX7
PACSIN2
PADI2
PALM
PDE4A
PDZD2
PGM1
PHKA1
PHOSPHO1
PIK3AP1
PIK3CB
PIK3R6
PKD2
PKP2
PKP4
PLCG2
PLCL2
PLEK
PLTP
PMEPA1
PNPLA7
PPM1H
PPP1R3B
PPP2R2C
PPP2R5C
PPP3CC
PRDM1
PRF1
PRR5
PRR5L
PTPA3
PTPN11
PTPN12
PTPN22
PTPN4
PTPN5
PTPRJ
PYGL
RAB11FIP4
RAB20
RACGAP1
RAI14
RASGRF1
RASGRF2
RASL11B
RCN1
RFC2
RGS1
RHOB
RHOC
RIN3
RIPPLY3
RNF149
RNF169
RNF180
RNF19B
RPTOR
RRAS2
RTN4RL1
RUNX3
S100A1
S1PR3
SC4MOL
SCIN
SCLY
SEC14L1
SELENBP1
SELENBP2
SELM
SERPINA3F
SERPINB6A
SFT2D2
SH2D1B1

SAMD9L
SASH3
SASS6
SCARB2
SCML4
SCRN3
SEC24A
SELL
SEMA4A
SETBP1
SGK1
SGK3
SH2D1A
SH2D1B2
SH2D3C
SH3BP2
SIDT1
SIKE1
SIRT3
SLAMF6
SLC12A7
SLC14A1
SLC26A11
SLC9A7
SLCO3A1
SLFN1
SLFN2
SLFN8
SLFN9
SMEK2
SNAI3
SNAPC3
SOAT2
SP100
SPATA13
ST3GAL4
ST8SIA4
STIM2
STK38
STYK1
SULF2
SYTL2
TBC1D10C
TBC1D2B
TBRG3
TGFB3
TGFBR1
TIRAP
TLR4
TM6SF1
TMEM163
TMEM165
TNFRSF13C
TNFRSF26
TNFSF8
TPM1
TRAF3IP3
TRAT1
TREML2
TRIM21
TTC13
TTC9C
TUBGCP5
TXNIP
TYROBP
UBASH3A
UGCG
VEGFC
VIPR1
WIPF1
WWP1
XAF1
XCL1
XRN2
XYLT1
ZBTB8A
ZC3H12D
ZDHHC15
ZFP157
ZFP260
ZFP273
ZFP277
ZFP418
ZFP422
ZFP512
ZFP563
ZFP597
ZFP7
ZFP709
ZFP71-RS1
ZFP719
ZFP759
ZFP760
ZFP763
ZFP825
ZKSCAN3
ZYX

SERPINB6A
SERPINB6B
SERPINB9
SERPINE2
SESTD1
SGTB
SLC16A10
SLC16A6
SLC22A15
SLC31A1
SLC35B1
SLC41A3
SLC6A20A
SLC7A6OS
SLC7A7
SLC9A2
SMAP2
SMOX
SMYD2
SNTB1
SNX18
SPRED2
SPSB1
SQLE
SRGAP2
SSX2IP
ST14
ST3GAL3
ST6GALNAC6
STAP1
STOM
STX11
SUMO1
SUSD2
SUSD3
TACSTD2
TCEAL1
TCN2
TCP11L2
TDRD3
TDRKH
THY1
TIFA
TIMP2
TIPRL
TLCD1
TMEM123
TMEM149
TMEM154
TMEM176A
TMEM176B
TMEM5
TMEM59
TMTC2
TNF
TNFRSF21
TNS3
TNS4
TOR1AIP1
TOX
TRF
TRP53INP1
TTLL1
TTYH2
TXNDC12
UBE2B
UBE2J1
UCP3
UPP1
VAMP4
VAV3
VDR
VEGFA
VPS37A
WARS
WBP1
WDR90
WIPI1
XKRX
ZBTB25
ZDHHC14
ZFP414
ZFP462
ZFP67
ZMAT4

PGLYRP1
PHF11
PIK3R5
PION
PLA2G4B
PLD3
PLEK
PLSCR4
PNRC2
POGK
POLE2
POLR3K
POT1A
POT1B
PPARGC1A
PPM1J
PQLC3
PRF1
PRKCB
PRKCQ
PRR5L
PSIP1
PTCD2
PTER
PTP4A3
PTPN12
PTPN4
PTPRC
PTRH2
PXMP3
PYCARD
PYHIN1
QRFP
RAB31
RAB7L1
RAC3
RACGAP1
RAP1A
RAP1GAP2
RAP2B
RAPH1
RASA1
RASA3
RASGEF1A
RASGRP2
RASL12
REEP5
RELT
RHOQ
RNF157
RNF216
RPA2
RPGR
RPL38
RRAGB
RRAS2
RSL1
S100A6
S1PR1
S1PR4
S1PR5
SAMD3
SAMD9L
SAP18
SASS6
SCARB2
SCD2
SCRN3
SEC61B
SELL
SEMA4A
SERPINB9B
SETBP1
SGK1
SGK3
SH2D1A
SH2D1B1
SH2D1B2
SH2D3C
SH3BP2
SIDT1
SIKE1
SLAMF6
SLC12A7
SLC14A1
SLC25A30
SLC37A2
SLC41A2
SLC9A7
SLFN2
SLFN8
SLFN9
SNAPC3
SNAPIN
SNX10
SNX11
SOAT2
SORD
SP100
SPATA13
SPN
SRPX
ST3GAL4
ST5
STEAP3
STIM2
STK32C
STK38
STYK1
SULF2
SYNE2
SYPL
SYT11
SYTL2

GIMAP4
GIMAP5
GIMAP6
GIMAP7
GIPC1
GLA
GLG1
GLRX
GLTP
GM12070
GM12185
GM12250
GM14005
GM14085
GM16515
GM8979
GNAQ
GNB2
GNB5
GNG2
GPC1
GPLD1
GPNMB
GPR114
GPR141
GPR18
GPR55
GPT2
GRIN1
GRXCR2
GSTM4
GTF2I
GVIN1
GYG
GZMB
H1FX
H2-AB1
H2-D1
H2-K1
H2-M3
H2-Q10
H2-Q2
H2-Q7
H2-Q8
H2-T10
H2-T22
H2-T23
H2-T9
H2AFX
H2AFY
H2AFZ
HAAO
HACL1
HDAC7
HDGFRP3
HDHD3
HEATR5A
HEATR5B
HECTD1
HECTD2
HELB
HERC1
HEXB
HIBCH
HIC2
HIF1A
HK1
HLX
HMGCR
HMGCS1
HMOX1
HMX2
HN1
HNRNPUL1
HOPX
HPSE
HS3ST3B1
HSD17B7
HSPA13
HSPA2
HSPB11
HSPB6
I830012O16RIK
ICAM1
ID2
IDH1
IDI1
IER5L
IFI203
IFI204
IFI44
IFIH1
IFIT1
IFIT2
IFIT3
IFITM1
IFITM2
IFITM3
IFNG
IFNGR1
IFT20
IFT52
IFT80
IGF2BP2
IGF2BP3
IGFL3
IIGP1
IKZF1
IKZF2
IL12RB2
IL18R1
IL18RAP
IL1RL2
IL2RB

GATSL3
GEMIN8
GFI1
GGCX
GIGYF1
GLIPR2
GLTSCR1
GM12191
GM13051
GM13251
GM15760
GM2382
GM5134
GM5148
GM561
GM711
GM973
GM996
GMFG
GMIP
GNA15
GPBP1L1
GPM6B
GPR132
GPR137B-PS
GPR179
GPR97
GRAP
GRASP
GRIK5
GRIN2D
GRTP1
GSTM5
GZMA
H2-DMA
H2-DMB2
H2-KE6
H2-OA
H2AFJ
HADH
HC
HCST
HEMGN
HEXIM1
HGF
HIF3A
HIP1
HIST1H1C
HIST1H1D
HPGD
HPGDS
HPS3
HRH4
HS1BP3
HS6ST1
HSD11B1
HSD17B10
HSD17B11
HSD3B7
HSPA1A
HUNK
ICA1L
ICAM2
ICOSL
IER2
IFFO1
IFI30
IFLTD1
IFNGR2
IKBKB
IKBKE
IL17RB
IL19
IL24
IL27RA
IL4
IL4RA
IL9R
IMPACT
INADL
INPP4B
INPP5D
IRAK3
IRF6
IRF9
IRS2
ISCA1
ITGA7
ITGB3
ITGB7
ITPKB
ITPR1
ITSN2
IZUMO4
JDP2
JMJD4
JUND
KBTBD3
KCNA2
KCNH2
KCNK5
KCNN4
KCTD12
KDM4A
KDM6B
KDSR
KIFC2
KLF2
KLF3
KLHDC1
KLHDC2
KLHL21
KLHL32
KLHL35

COX7A1
CPD
CPE
CPEB3
CPNE2
CPNE8
CPOX
CPSF2
CPT1C
CRABP2
CRAMP1L
CRLS1
CRTAM
CRTC3
CRY1
CSAD
CSE1L
CSPG5
CSRNP2
CSTF3
CTBP2
CTDSPL
CTH
CTLA2B
CTNNAL1
CTNND1
CTPS
CTSC
CTTNBP2NL
CUBN
CUL1
CUL7
CUX1
CWC22
CWC27
CWH43
CX3CR1
CXCR5
CYB5
CYP1A1
CYP1B1
D11WSU47E
D19BWG1357E
D630003M21RIK
D630045J12RIK
D930048N14RIK
DAB2
DACT3
DALRD3
DARS2
DBH
DBR1
DCBLD2
DCDC2C
DCLK1
DCLRE1C
DCTD
DDHD1
DDI2
DDR1
DDX1
DDX11
DDX18
DDX21
DDX27
DDX31
DENND2C
DERL3
DGCR8
DGKG
DHFR
DHRS13
DHRS4
DHX15
DHX29
DHX33
DHX9
DIABLO
DIAP2
DIDO1
DIS3
DKC1
DLG2
DMWD
DMXL2
DNA2
DNAJA1
DNAJB5
DNAJC11
DNAJC2
DNAJC21
DNAJC27
DNAJC6
DNAJC9
DNM1L
DNM3
DNPEP
DNTT
DNTTIP2
DOCK3
DOCK4
DOCK6
DOT1L
DPF1
DPH5
DPM2
DPY30
DRG2
DRP2
DSCC1
DSEL
DSN1
DST
DSTYK

SNORD47
SNORD49A
SNORD49B
SNORD55
SNORD61
SNORD68
SNORD82
SNORD85
SNORD87
SNRPE
SNRPF
SOX4
SPINK5
ST8SIA1
ST8SIA6
STEAP3
STIL
STMN1
STYK1
TAF1D
TBC1D4
TCEAL3
TDGF1
TGM3
THBS1
TIPIN
TIRAP
TLR7
TMEM38B
TMEM48
TOP2A
TPX2
TREML2
TRIM36
TRIP13
TRPM6
TSPAN32
TTC39C
TWSG1
TXN1
UBE2V2
UCK2
UGCG
UHRF1
USMG5
VAULTRC5
VDR
WFIKKN2
ZBTB16
ZCWPW1
ZFP536

SH2D1B2
SH2D3C
SH3TC1
SIPA1L1
SLC26A10
SLC28A2
SLC35F5
SLC36A1
SLC38A8
SLC39A4
SLC46A3
SLC9A3R1
SNAP23
SNX18
SNX9
SOAT2
SPATS2
SPP1
SQLE
SREBF2
ST3GAL5
ST6GALNAC2
STARD4
STK32C
STK39
STXBP5
SULF2
SULT2B1
SUSD4
SYTL2
SYTL3
TBC1D24
TBX21
TCF4
TESC
TESK2
TEX2
TGFB3
TGM2
TIGIT
TIPARP
TM7SF3
TMCC3
TMEM149
TMEM38B
TMEM59L
TMPRSS6
TMTC4
TNFAIP3
TNFSF10
TNFSF13B
TNFSF8
TNKS1BP1
TRDN
TRIB1
TRIO
TSGA10
TSPAN9
TXK
TYROBP
UBAC2
UBE2L6
USP11
USP46
VAV3
VIPR2
VPS37B
ZBED3
ZBTB38
ZCCHC18
ZFP395
ZMAT4

TADA1
TAF1B
TBC1D10C
TBC1D2B
TIGIT
TIRAP
TLR4
TM6SF1
TM6SF2
TMEM163
TMEM165
TMEM171
TMEM37
TMSB15A
TNFRSF26
TRAF3IP3
TRAF5
TREML2
TRIM21
TRIM27
TRMT11
TSC22D1
TSPAN5
TSTD2
TTBK2
TTC39C
TWF2
TXNIP
TYROBP
UBA3
UBLCP1
UBXN2B
UGCG
UTP23
VEGFC
VTI1B
WIPF1
WTAP
XAF1
XRN2
YWHAQ
ZBTB8A
ZDHHC15
ZEB2
ZFP105
ZFP128
ZFP157
ZFP160
ZFP235
ZFP251
ZFP260
ZFP273
ZFP277
ZFP300
ZFP382
ZFP418
ZFP456
ZFP512
ZFP54
ZFP563
ZFP595
ZFP597
ZFP637
ZFP7
ZFP708
ZFP709
ZFP719
ZFP748
ZFP759
ZFP760
ZFP763
ZFP780B
ZFP825
ZFP85-RS1
ZFP87
ZFP873
ZKSCAN3
ZKSCAN6
ZYX
IL34
IL6ST
IMPA2
IMPAD1
INPP1
INSIG1
INSL6
IPCEF1
IQGAP1
IQSEC1
IRF2
IRF8
IRGM1
IRGM2
ISG15
ITGA2
ITGA6
ITGAL
ITGAM
ITGAV
ITGB5
ITIH5
JARID2
JUN
KATNAL1
KATNB1
KCNAB3
KCNC1
KCNJ8
KCNK7
KCTD7
KDELC2
KHDRBS1
KIF14
KIF1A
KIF2A
KIF3C
KIF9
KIT
KITL
KLF6
KLF7
KLHL25
KLHL4
KLHL6
KLRB1F
KLRC1
KLRD1
KLRK1
LAG3
LAMA5
LAMB3
LAMC1
LASP1
LAT2
LBH
LCA5
LCN4
LDLR
LFNG
LGI4
LILRB4
LIMS1
LIN7C
LIPA
LITAF
LNPEP
LPIN1
LPIN2
LRMP
LRP12
LRRC38
LRRC8B
LRRC8C
LRRK1
LSR
LSS
LTA4H
LTB4R1
LTK
LY6A
LY6C1
LY6C2
LY6E
LY75
LYN
LYPD6B
LYRM1
LYSMD2
LYZ2
LZTS1
MAML3
MAN1A
MAN2B2
MAP1LC3A
MAP2K5
MAP3K5
MAP3K8
MAP4K5
MAPK3
MAPRE1
MAPRE3
MATN2
MBNL1
MCTP2
MEF2A
METTL9
MFSD6
MGAM
MGST2
MID1IP1
MLKL
MORN4
MOSPD2
KLK8
KPNA4
KRBA1
KREMEN2
KRT18
KRT80
L1CAM
LAIR1
LAMP1
LAPTM4B
LCMT1
LDB1
LEFTY1
LEMD2
LEPROT
LGALS7
LGMN
LHFP
LIMD1
LLGL2
LMBR1L
LMBRD1
LPAR2
LPAR5
LPCAT4
LRRC32
LRRC8A
LSM1
LSP1
LUM
LY6G5B
LYNX1
LYPLA2
LYRM5
LYRM7
MAN1C1
MAN2B1
MANSC1
MAP1LC3B
MAP2K6
MAP3K15
MAP3K2
MAP3K9
MAP4K2
MAPK1IP1
MAPRE2
MAST3
MAST4
MATK
MBOAT1
MCL1
MCTP1
MCTS2
MDP1
MED26
MEPCE
METRNL
METTL8
MFNG
MGAT3
MGMT
MICALL1
MICALL2
MIDN
MIRLET7B
MLLT3
MLYCD
MOSPD3
MOXD1
MPL
MRPL35
MRPL55
MRPS12
MRPS24
MTG1
MTMR10
MUC19
MXD4
MYEOV2
MYO6
MYO9B
N6AMT1
NAB1
NAGA
NBEAL2
NCEH1
NCKAP5L
NCLN
NCOA3
NCOA7
NDFIP1
NDUFA6
NEU1
NFE2
NFIA
NFIL3
NFX1
NIPAL1
NPM3
NPTN
NR1D2
NRBP2
NRGN
NRIP1
NRP2
NSMCE1
NTRK3
NUDT19
NUFIP2
OAS1B
OAS1C
OAS2
OLFR60
ORAI2
DTL
DTYMK
DUS4L
DUSP4
DYRK3
DYRK4
DZIP3
E130308A19RIK
E2F3
E2F6
E2F8
E330020D12RIK
EBF1
EBNA1BP2
EEA1
EFCAB5
EFCAB7
EFTUD2
EGR2
EGR3
EHBP1
EHD4
EIF2AK4
EIF2B3
EIF3B
EIF4A1
EIF4G1
EIF5A
ELK3
ELP4
EML4
EMP1
ENDOD1
ENO2
ENPP2
ENY2
EPB4.1L2
EPN2
EPRS
ERC1
ERH
ERMAP
ERV3
ESF1
ETV1
EVPL
EXO1
EXOC6B
EXOSC2
EXOSC7
EXOSC8
EXT1
EZH2
F3
F730043M19RIK
FABP4
FABP5
FAM107A
FAM124B
FAM129B
FAM131B
FAM133B
FAM135A
FAM161B
FAM184B
FAM193A
FAM20C
FAM53B
FAM57A
FAM73B
FAM83D
FAM83E
FAM98A
FANCA
FANCB
FANCG
FANCI
FANCM
FARSB
FASTKD3
FBL
FBXL12
FBXL19
FBXO2
FBXO5
FBXW7
FCRL1
FEN1
FERMT1
FGD1
FGF13
FGF2
FGFR1OP
FIGNL1
FIP1L1
FJX1
FKBP1A
FKBP1B
FKTN
FLNB
FNBP1L
FNDC3B
FNIP2
FOXD2
FOXF2
FOXP3
FPGS
FRMD4A
FRMD5
FRMD6
FSCN1
FSD1L
FSTL4
FTSJ3

MPP1
MPZL2
MPZL3
MRVI1
MS4A4B
MS4A4C
MS4A4D
MS4A6D
MSH5
MSMB
MT1
MT3
MTHFD2
MTMR6
MUC13
MVD
MVK
MXD1
MXRA8
MYADM
MYCN
MYD88
MYO1E
MYO1F
MZT2
NAA50
NAB2
NACC2
NAPRT1
NCALD
NCAPH2
NCF1
NDN
NDRG1
NDRG2
NDRG3
NEB
NEDD4
NEIL1
NGLY1
NICN1
NIPA1
NKG7
NLRC5
NLRP1A
NLRP1B
NLRP3
NMNAT2
NOD1
NOXO1
NPHP4
NR2F6
NRM
NRN1
NSDHL
NSG2
NUAK2
NUCB1
NUCKS1
NUDT21
NUDT4
NUMBL
NXNL2
NXT2
OAS3
OASL2
OBFC1
OGFRL1
OLFM1
OSBPL8
OTUD7B
P2RX3
P2RY14
P4HA1
P4HA2
PADI2
PAK6
PAOX
PAPSS1
PAQR7
PARD6A
PARP12
PARP14
PARP8
PARVG
PBX4
PCBP4
PCCA
PCYT1A
PDE2A
PDE5A
PEA15B
PGM2
PHF11
PHLPP1
PHYH
PI4KB
PICALM
PIGZ
PIK3AP1
PIK3R5
PIM2
PKD1L2
PKIB
PKIG
PLAC8
PLAT
PLCG2
PLCL2
PLD2
PLD4
PLEKHH3
PLEKHM3
PML
ORC4
OSBPL7
OTUD1
OXCT1
P2RX4
P2RX7
P2RY1
P2RY10
PADI4
PANX1
PARD6B
PAX9
PCF11
PCGF2
PDCD2
PDCD4
PDE4A
PDLIM2
PDLIM4
PDX1
PDZRN3
PEPD
PEX19
PFDN5
PHF1
PHLDA3
PHLDB1
PHLDB3
PIGM
PIM3
PIP5K1B
PIP5K1C
PISD-PS1
PJA1
PLA2G12A
PLA2G6
PLCB4
PLCD1
PLCL1
PLXDC1
PLXDC2
PLXNA1
PMM2
PNKP
PNPLA7
PNPO
PNRC1
PNRC2
PODNL1
POGZ
POLE4
POLM
POLR1A
PON3
PORCN
POT1B
POU4F1
PPARG
PPCS
PPP1R11
PPP1R15A
PPP1R9B
PPP2R3A
PPP2R5A
PPP3CC
PQLC1
PRKAG1
PRKCQ
PRKCZ
PRKD2
PRKD3
PRKDC
PRODH
PROS1
PRR13
PRR14
PRSS32
PSEN2
PTGER2
PTGIR
PTPN13
PTPN18
PTPN7
PTPRCAP
PYCARD
PYGM
QPRT
QRFP
RAB19
RAB20
RAB32
RAB37
RAB3A
RAB4A
RABAC1
RAMP3
RANBP6
RAP1B
RAP1GAP
RAP1GAP2
RAP2B
RAPGEF5
RAPSN
RARA
RASA3
RASAL3
RASGRP1
RASGRP2
RASGRP4
RASSF5
RASSF8
RBAK
RBM12B
RCHY1
FTSJD2
FUBP1
FUS
FUT10
FUT7
FXR2
FZD7
GABARAPL1
GABRR2
GAD2
GADD45A
GALM
GALNT14
GAN
GAP43
GAR1
GART
GAS5
GATAD2B
GATM
GCLM
GCNT2
GCSH
GDF6
GDPD5
GEMIN4
GEMIN6
GFM1
GFOD1
GFPT2
GGA2
GINS1
GINS3
GJA3
GJA5
GK5
GKAP1
GLCCI1
GLCE
GLI3
GLS2
GM10033
GM10069
GM10845
GM13034
GM3002
GM5124
GM5177
GM527
GM5434
GM5643
GM5803
GM6642
GM6682
GM7102
GM8994
GMNN
GNA12
GNL2
GNL3
GOLGA1
GOLGA4
GOLIM4
GOLM1
GPATCH4
GPD2
GPR125
GPR15
GPR162
GPR65
GPRASP2
GPS1
GRHL1
GRIA3
GRK1
GRK4
GRWD1
GSG1L
GSG2
GSPT1
GTF2F2
GTF2H5
GTF2IRD1
GTSE1
H19
HAP1
HARS
HAS3
HAUS1
HAUS4
HAUS5
HAUS6
HAX1
HCFC1
HCFC2
HCN3
HDAC2
HEATR3
HECW2
HELLS
HELQ
HIC2
HIRA
HIRIP3
HIST1H3E
HIST1H4K
HIST2H2BB
HIST2H4
HIVEP3
HMBOX1
HMGB1-RS17
HMGB3
HMGN1
HMGN3

PMVK
POR
POU6F1
PPM1H
PPM1J
PPP1R12A
PPP1R3B
PRCP
PRDM1
PRDX4
PRELID1
PRELID2
PRF1
PRKCA
PRKCE
PRNP
PRPF18
PRPH
PRR5
PRR7
PRRC1
PRRG4
PRSS16
PRSS35
PSG17
PSMB8
PSMB9
PTDSS2
PTEN
PTGER3
PTMS
PTPN14
PTPN22
PTPN5
PTPRE
PVR
PXMP4
PXT1
PYGL
PYHIN1
QARS
RAB27B
RAB28
RAB31
RAB3D
RAP2A
RAPGEF4
RASA4
RASGRF2
RASL11A
RASSF3
RASSF4
RBMS2
RBPMS
RC3H2
RCN1
RCN2
RDH11
RDM1
RECK
RELL1
RET
RFK
RFX2
RGAG4
RGS3
RHOB
RHOC
RILPL2
RIMS2
RIN3
RIOK1
RNF130
RNF141
RNF157
RNF26
ROPN1L
RPA1
RPGRIP1L
RRAS
RRAS2
RSPH1
RSPH9
RTBDN
RTN3
RTP4
RUFY4
RUNX3
RYR1
S100A11
S100A4
SAMHD1
SAP30L
SCARB2
SCD1
SCD2
SCLY
SCPEP1
SCRN3
SCRT1
SDC3
SDCBP2
SELL
SEMA3B
SEMA3F
SEMA4A
SEMA4G
SEPN1
SERPINB5
SERPINB6A
SERPINB6B
SERPINB9
SERPINE2
SETD7
RDH10
REC8
RERE
RGL2
RGS1
RGS14
RHBDL1
RING1
RLTPR
RNF111
RNF123
RNF128
RNF144A
RNF152
RNF167
RNF19B
RNF217
ROM1
RPL12
RPL13A
RPL14
RPL17
RPL18
RPL19
RPL22
RPL22L1
RPL27
RPL27A
RPL32
RPL34
RPL36
RPL36AL
RPL37A
RPL38
RPL39
RPL9
RPLP1
RPLP2
RPS10
RPS12
RPS13
RPS14
RPS15A
RPS18
RPS19
RPS21
RPS23
RPS24
RPS27A
RPS27L
RPS28
RPS3
RPS6KA5
RPS6KL1
RPS7
RREB1
RTF1
RTN4RL1
RUNX1
RUSC1
RXRB
RYR3
S100A1
S100A13
S100A6
S1PR1
S1PR4
SAG
SAMD9L
SARS2
SATB1
SAV1
SBF1
SCAI
SCAND1
SDF2
SEC16B
SEC61B
SELM
SEMA4B
SEMA4F
SEMA6C
SEPP1
SERPINF1
SEZ6L2
SFT2D2
SGCE
SGMS1
SGSH
SH3TC1
SIGIRR
SIKE1
SIPA1L3
SIRT5
SIRT7
SIT1
SLA
SLC10A3
SLC12A5
SLC12A9
SLC16A2
SLC17A6
SLC17A9
SLC25A37
SLC25A45
SLC26A11
SLC27A1
SLC29A4
SLC2A6
SLC35B4
SLC35C1
SLC35C2
SLC36A1
SLC37A1
HMGN5
HN1L
HNRNPA2B1
HNRNPD
HNRNPH1
HNRNPL
HNRNPM
HOOK1
HOOK2
HSF2
HSF2BP
HSP90AA1
HSPA4L
HSPA9
HSPD1
HSPH1
HTRA2
HTT
HUS1
HYOU1
IARS
IBTK
ICA1
ID1
IDE
IDI2
IFRD2
IFT74
IGF1R
IGLON5
IGSF3
IKZF3
IKZF4
IL17RC
IL17RE
IL1F9
IL1R1
IL1RN
IL21
IL23R
IL2RA
IL9
ILTIFB
IMPG2
INPP5F
INTS10
INTS2
INTS4
INTS7
INTU
IPMK
IPO4
IPO5
IPO9
IQCB1
IRAK1BP1
IRF4
IRGQ
ISCA2
ITGA3
ITGA5
ITPA
ITPR3
IVNS1ABP
IWS1
JAM3
JMJD1C
JMJD6
JMY
JPH4
JUP
KANK3
KAT5
KCNC3
KCNH5
KCNIP2
KCNMB4
KCTD11
KCTD14
KDELC1
KDM2B
KIF1B
KIF20B
KIF3B
KIF4
KIF5C
KIFAP3
KIFC3
KLC1
KLHL12
KLHL23
KLHL8
KLRC2
KLRC3
KLRG2
KNG2
KPNA2
KRT6B
KTN1
L2HGDH
L7RN6
LAMC2
LAMP3
LAP3
LARP1
LARP7
LARS2
LAS1L
LBP
LDHB
LDLRAD3
LENG8
LEO1
LEPRE1

SGIP1
SH3BP2
SH3BP5
SH3GLB1
SHF
SHISA2
SIAH3
SIPA1L1
SKAP2
SLAMF1
SLAMF7
SLC11A2
SLC12A8
SLC16A1
SLC20A1
SLC25A1
SLC25A23
SLC25A24
SLC25A30
SLC30A4
SLC35F5
SLC46A3
SLC7A3
SLC7A5
SMAGP
SMCHD1
SMPDL3A
SNAI3
SND1
SNTB1
SNTB2
SNX10
SNX18
SNX9
SORCS2
SORD
SOS2
SP100
SP110
SP140
SPARC
SPATA13
SPATA6
SPRED2
SPRY2
SPRYD4
SPT1
SPTY2D1
SQLE
SSBP2
SSR1
SSRP1
ST14
ST3GAL4
ST3GAL6
ST8SIA1
STAP1
STARD4
STAT1
STIM2
STK17B
STK24
STK32C
STK39
STON2
STXBP5
STYK1
SUGT1
SULF2
SULT2B1
SUSD3
SWAP70
SYNE2
SYTL1
SYTL2
SYTL3
TAGLN2
TANC1
TAP1
TAX1BP1
TBC1D19
TBC1D22B
TBC1D2B
TBC1D30
TBKBP1
TBL1X
TBX21
TCP11L1
TET1
TGM1
TGTP1
THEMIS
THRA
THRB
TIFAB
TIRAP
TKT
TLE3
TMCO4
TMED10
TMED8
TMEM106A
TMEM107
TMEM108
TMEM143
TMEM151B
TMEM158
TMEM159
TMEM163
TMEM170B
TMEM180
TMEM205
TMEM26
TMEM30A
SLC37A3
SLC38A9
SLC39A11
SLC39A6
SLC39A7
SLC41A2
SLC41A3
SLC4A4
SLC4A7
SLC8A3
SLC9A6
SLC9A8
SLCO4A1
SLFN2
SLFN5
SMAD5
SMG7
SNAP47
SNAPC4
SNRPG
SNX33
SOCS1
SORBS3
SP6
SPATC1
SPATS2L
SPCS3
SPINT2
SPR
SPSB1
SPTLC3
SRGN
SRPK1
SSR4
ST3GAL1
ST3GAL5
ST6GAL1
ST6GALNAC1
ST8SIA4
ST8SIA6
STBD1
STC1
STK11IP
STK38
STX1A
SUFU
SUN1
SUPT3H
SUV420H1
SV2C
SVAL1
SYPL
SYS1
SZT2
TAF1C
TANC2
TAZ
TBC1D10A
TBC1D2
TBCD
TBRG1
TBX6
TCIRG1
TCTN3
TDGF1
TDRKH
TEP1
TESC
TET2
TEX264
TGFB1I1
THY1
TIGIT
TIMM10
TJP3
TK2
TKTL1
TLR1
TM2D1
TM2D3
TMC6
TMC8
TMEM141
TMEM160
TMEM161B
TMEM185B
TMEM191C
TMEM208
TMEM221
TMEM223
TMEM41B
TMEM50A
TMEM60
TMEM63A
TMEM64
TMEM81
TMEM87B
TMIE
TMSB4X
TMUB1
TNFAIP3
TNFSF13B
TNFSF8
TNP2
TOB1
TOMM20
TOMM34
TPP1
TPRGL
TRAF5
TRAT1
TRIAP1
TRIB3
TRIM16
LGR4
LHX6
LIF
LIG1
LIPG
LIPT2
LMLN
LMNA
LMO4
LOC380994
LONP1
LONP2
LONRF3
LOXL2
LPGAT1
LPXN
LRFN4
LRIG1
LRP1
LRP2BP
LRPPRC
LRRC49
LRRC58
LRRC59
LRRC7
LRRK2
LSM14B
LSM3
LTA
LTV1
LUC7L3
LUM
LUZP1
LY6K
LYAR
LYRM4
LZIC
LZTS2
MAD1L1
MAFF
MAGED1
MAGED2
MAGI3
MAGOH
MALAT1
MALT1
MAML2
MAOA
MAP2K3
MAP3K7
MAPK8
MAPKAPK3
MAPKAPK5
MAPKBP1
MARCKSL1
MARVELD1
MAST2
MAT2A
MC2R
MCM10
MCM2
MCM3
MCM4
MCM5
MCM6
MCM8
MDFIC
MDN1
ME2
MEAF6
MECR
MED14
MED18
MEGF11
MEGF8
METAP1D
METTL1
METTL13
MEX3A
MEX3C
MFHAS1
MFSD2A
MFSD2B
MFSD7B
MFSD7C
MGAT5
MGST3
MIB1
MICAL2
MICAL3
MID1
MID2
MIF4GD
MIR17HG
MIR615
MKI67
MLF1
MLH1
MLLT1
MMP11
MORC2A
MORF4L2
MOV10
MPHOSPH10
MPHOSPH6
MPZL1
MRPL37
MRPL38
MRPL42
MRPL45
MRPL47
MRPS10
MRPS22
MRPS27

TMEM45A
TMEM51
TMEM66
TMEM71
TMEM9
TMOD3
TNFRSF1A
TNFRSF1B
TNFRSF9
TNFSF10
TNKS1BP1
TNS1
TNS4
TPD52
TPP2
TPST2
TRAF1
TRAFD1
TREX1
TRIB2
TRIM12A
TRIM13
TRIM14
TRIM30A
TRIM36
TRIM46
TRIM59
TRP53INP1
TSPAN3
TSPAN31
TTC39B
TTC7B
TTLL12
TTYH3
TUBA1A
TUBA1B
TUBA1C
TUBA8
TUBB5
TUBD1
TULP4
TUSC3
TXK
TXNDC16
UBAC2
UBE2C
UBE2F
UBE2H
UBE2L6
UBE2S
UEVLD
UGCG
UHRF1BP1L
UNC119B
UNC93B1
USP12
USP18
USP3
VARS
VAV2
VCAN
VIPR1
VOPP1
VPS13A
VPS37B
VPS8
VWA5A
WBP5
WDR19
WDR31
WDR44
WDR78
WDR82
WDTC1
WNK1
WNK2
WRN
XCR1
XDH
XKR5
XPR1
YIPF4
YPEL4
YWHAG
ZBP1
ZDHHC21
ZEB2
ZFP287
ZFP36L1
ZFP395
ZFP608
ZKSCAN17
ZNRF2
ZYG11B
TRIM39
TRIM65
TRIM8
TRIP6
TSHZ3
TSPAN17
TSPAN32
TSPAN9
TTC28
TUBA4A
TUG1
UAP1L1
UBA52
UBL3
UBXN6
UCP2
ULK3
UNC119
UNC5A
UQCRH
USE1
USP20
UVRAG
VAMP5
VAMP8
VILL
VKORC1
VMAC
VPS11
VPS33B
WDFY2
WDR12
WDR26
WDR41
WDR6
WDR81
WFIKKN2
WNT9A
XLR3B
XLR4B
XLR4C
XPC
YOD1
YPEL3
YTHDF3
ZADH2
ZBTB10
ZBTB37
ZBTB6
ZFAND2B
ZFHX2
ZFP109
ZFP160
ZFP182
ZFP263
ZFP273
ZFP280B
ZFP316
ZFP317
ZFP36
ZFP362
ZFP36L2
ZFP40
ZFP420
ZFP442
ZFP456
ZFP467
ZFP472
ZFP51
ZFP551
ZFP558
ZFP579
ZFP646
ZFP654
ZFP658
ZFP677
ZFP68
ZFP703
ZFP707
ZFP709
ZFP746
ZFP773
ZFP777
ZFP780B
ZFP784
ZFP827
ZFP831
ZFP84
ZFP865
ZGPAT
ZMYND8
ZRSR1
ZSCAN10
ZSCAN22
MRPS5
MRPS6
MRRF
MRTO4
MS4A8A
MSC
MSH6
MSL3
MSRB3
MST1
MTBP
MTCP1
MTHFD1
MTHFD2L
MTHFSD
MTMR11
MTO1
MTOR
MTSS1
MTX1
MTX2
MUC6
MURC
MYB
MYBBP1A
MYBL2
MYEF2
MYH11
MYO10
MYO19
MYO1C
MYO1D
MYO3B
MYO5A
MYO9A
N4BP1
N4BP3
NAA15
NAA16
NAA25
NAA35
NAA40
NAF1
NARS2
NASP
NAT10
NAV1
NAV2
NBN
NCBP1
NCBP2
NCKAP1
NCLN
NCS1
NDEL1
NDST1
NDUFA12
NDUFA5
NDUFAF2
NDUFAF4
NDUFC1
NEDD8
NEFH
NEIL3
NEK6
NEK8
NELF
NETO2
NEU3
NFAT5
NFE2L3
NFIX
NFKB1
NFKB2
NFKBIA
NFKBID
NFKBIZ
NFXL1
NHS
NHSL1
NIF3L1
NINJ1
NINL
NKD2
NKRF
NMD3
NME1
NME4
NME6
NMT2
NNT
NOC3L
NOC4L
NOL10
NOL11
NOL8
NOLC1
NOM1
NOP14
NOP16
NOP2
NOP58
NOV
NPAS4
NR1D1
NR4A1
NR4A2
NR4A3
NR6A1
NRARP
NRD1
NRIP3
NSF
NSFL1C

NSMCE4A
NSUN2
NSUN4
NT5DC3
NT5E
NUAK1
NUCB2
NUDC
NUDCD1
NUDT1
NUDT5
NUF2
NUP133
NUP155
NUP205
NUP210L
NUP43
NUP54
NUP85
NUP88
NUP93
NUP98
NUTF2
NYNRIN
OAZ3
OCIAD2
OCRL
ODC1
ODF2L
OGDHL
OLFR1033
OLFR856-PS1
OPTN
ORC1
ORC2
ORC6
ORM2
OSBPL11
OSGEPL1
OSGIN2
OTUD6B
PA2G4
PABPN1
PAK1IP1
PALB2
PANK4
PAPD7
PAPSS2
PAQR8
PARD6G
PARP1
PARP2
PAXIP1
PCBP3
PCDH7
PCGF6
PCNT
PDAP1
PDCD1
PDCD11
PDCD5
PDE4C
PDE6D
PDGFB
PDGFC
PDIA2
PDIA5
PDIA6
PDK3
PDLIM5
PDPN
PDXDC1
PDZD4
PDZK1
PECR
PELI2
PELP1
PER2
PERP
PFAS
PFDN1
PFDN4
PFKFB1
PHACTR2
PHACTR4
PHB
PHF14
PHTF2
PIAS2
PID1
PIGG
PIGL
PIK3C2B
PIK3R1
PIK3R3
PIN4
PINX1
PIPOX
PITPNM2
PKHD1L1
PLA2G4C
PLAGL1
PLAGL2
PLEKHA1
PLEKHA8
PLEKHB1
PLEKHB2
PLEKHF2
PLEKHG4
PLEKHO1
PLOD2
PLS1
PLS3
PLSCR1

PLSCR4
PLXNA3
PLXNB1
PMEPA1
PNCK
PNMA1
PNN
PNO1
PNPT1
POGK
POLA2
POLD3
POLE
POLE3
POLQ
POLR1B
POLR2K
POLR3D
POLR3G
POP1
POP4
POU2AF1
PPA1
PPAPDC1B
PPFIA3
PPFIBP1
PPID
PPM1F
PPME1
PPP1CC
PPP1R12B
PPP1R3C
PPP1R3D
PPP1R8
PPP2R1B
PPP4R4
PPRC1
PPTC7
PRDM10
PRDM4
PRDM5
PRIM1
PRKAR1B
PRKCI
PRKRIR
PRLR
PRMT1
PRMT5
PRMT7
PROCA1
PRPF19
PRPF3
PRPF31
PRPF38B
PRPF4B
PRPS1
PRR18
PRR5L
PRRT2
PRSS12
PSD3
PSMC1
PSMC2
PSMC4
PSMC5
PSMD1
PSMD12
PSMD6
PSMD7
PSME3
PSPC1
PSTPIP2
PTCD3
PTGER4
PTGFRN
PTK2
PTK7
PTOV1
PTPN1
PTPN23
PTPRF
PTPRJ
PTPRS
PUS10
PUS7
PWP1
PWWP2A
PWWP2B
PYCRL
PYROXD2
QRSL1
QSER1
QSOX2
QTRTD1
R3HDM1
RAB11FIP3
RAB23
RAB26
RAB38
RAB3IP
RABGGTB
RABL2
RAC3
RAD1
RAD50
RAD51AP1
RAD52
RAD54B
RAD54L
RAD54L2
RALGPS1
RANBP1
RANGRF
RARB

RARG
RARS
RARS2
RASA1
RASAL2
RASGEF1B
RASGRP3
RASL11B
RBBP7
RBBP8
RBFOX2
RBM17
RBM18
RBM19
RBM25
RBM28
RBM4B
RBMX
RBMX2
RBP4
RCAN1
RCAN3
RCCD1
RCL1
RDH11
RDX
RECQL4
REEP1
REEP2
RELB
REP15
REV1
REXO2
REXO4
RFC3
RFX5
RFX8
RGAG4
RGMB
RGS16
RGS2
RHEBL1
RHOT1
RIF1
RIN2
RIOK2
RMRP
RNASEH2B
RNF149
RNF19A
RNF208
RNF216
RNF8
RNFT1
RNFT2
RNMT
RNMTL1
RNPS1
RNU12
ROCK2
RORA
RORC
RPAP3
RPP30
RPRD1A
RPS27L
RPS6KC1
RPUSD2
RRAGA
RRAGD
RRP1
RRP12
RRP15
RRP1B
RRP9
RSAD1
RSL1D1
RSRC2
RTEL1
RTKN
RTN2
RTN4IP1
RUFY1
RUFY3
RUVBL1
RUVBL2
RYBP
S100PBP
SAP30
SARNP
SASS6
SBK1
SCARNA17
SCLT1
SCN1B
SCN4B
SCRIB
SDAD1
SDC1
SDC2
SDHAF1
SEC1
SEC24A
SEC61A2
SELP
SEMA3D
SEMA6D
SEMA7A
SERF1
SERINC5
SERP2
SERPINE1
SERTAD4
SET

SETD6
SF3A3
SFPQ
SFRP2
SGK1
SGOL1
SH3BGRL2
SH3BP4
SH3PXD2B
SH3RF1
SHB
SHMT1
SHMT2
SHQ1
SIAH1A
SIAH1B
SIGMAR1
SIM2
SKI
SKIV2L2
SKP2
SLC12A2
SLC15A3
SLC16A10
SLC16A4
SLC18A2
SLC19A1
SLC19A2
SLC1A4
SLC22A17
SLC25A13
SLC25A15
SLC25A18
SLC25A19
SLC25A27
SLC25A42
SLC27A6
SLC29A1
SLC29A2
SLC34A3
SLC35D3
SLC37A2
SLC38A6
SLC39A1
SLC39A10
SLC39A14
SLC41A1
SLC43A1
SLC43A3
SLC44A1
SLC46A1
SLC4A11
SLC4A2
SLC4A8
SLC5A3
SLC7A14
SLC7A6
SLC9A5
SLC9A7
SLC9A9
SLFN10-PS
SLMO2
SLTM
SMARCAD1
SMARCC1
SMARCE1
SMG5
SMGC
SMN1
SMPD4
SMYD2
SMYD5
SNHG1
SNHG8
SNORA21
SNORA3
SNORD104
SNRNP70
SNRPA1
SNRPD1
SNX16
SNX27
SOCS2
SORBS1
SORT1
SOX12
SOX4
SPAG1
SPATA5
SPDEF
SPECC1
SPG20
SPINT1
SPIRE1
SPON1
SRC
SRD5A1
SRL
SRM
SRRT
SRSF10
SSB
SSBP1
SSX2IP
ST13
ST3GAL3
ST5
ST6GALNAC3
ST6GALNAC4
ST7
STARD13
STARD7
STAT3
STAT5A

STIP1
STK35
STK38L
STON1
STX11
STX12
STXBP3A
STXBP4
SULT1A1
SUPT16H
SUPV3L1
SUV39H1
SUV39H2
SYCE2
SYDE2
SYN3
SYNCRIP
SYNGR2
SYP
SYT11
TADA2A
TAF1D
TAF4B
TAF9
TALDO1
TANC2
TARDBP
TARS
TARSL2
TBC1D16
TBC1D24
TBC1D30
TBCE
TBL3
TCEA2
TCERG1
TCF19
TCF7L1
TDP2
TDRKH
TEAD3
TEC
TECPR2
TERF2
TFDP1
TFDP2
TFF1
TFRC
TGFBI
TGFBR1
TGIF1
TGM2
TGS1
THG1L
THOP1
TIA1
TICAM2
TIMD2
TIMELESS
TIMM17A
TIMM17B
TIMM23
TIMM44
TIMM50
TIMM8A1
TIMM9
TIMP1
TIPIN
TJP2
TLCD1
TLE2
TLN2
TM9SF1
TM9SF4
TMCC2
TMEFF1
TMEM120B
TMEM131
TMEM132A
TMEM136
TMEM144
TMEM17
TMEM176B
TMEM190
TMEM201
TMEM216
TMEM55B
TMEM63B
TMEM86B
TMTC2
TMTC3
TMTC4
TNF
TNFAIP1
TNFRSF10B
TNFRSF13B
TNFRSF21
TNFRSF23
TNFRSF25
TNFRSF8
TNFSF4
TNIP1
TNIP2
TNIP3
TNK1
TNPO3
TOMM40
TOP1
TOP1MT
TOPBP1
TOX
TPD52L2
TPM1
TRA2A

TRAF3
TRAF3IP1
TRAF6
TRAIP
TRAP1
TRERF1
TRIM2
TRIM3
TRIM44
TRIP13
TRMT5
TRMT6
TRP53
TRPS1
TRUB1
TSC22D1
TSEN2
TSFM
TSKU
TSPAN2
TSPAN6
TSPYL2
TSR2
TTBK1
TTC21B
TTC27
TTC3
TTC8
TTI1
TTK
TTL
TTLL4
TUBB2B
TUBB6
TUBGCP3
TULP3
TXLNA
TXNRD1
TXNRD3
TYMS
TYR
TYRO3
U2AF1
UBA2
UBAP2
UBASH3B
UBE2CBP
UBE2E2
UBE2M
UBE2Q2
UBE4B
UBQLN4
UBR3
UBR4
UBR5
UBTD2
UCHL1
UCHL3
UCHL5
UHRF1
UHRF1BP1
UIMC1
UMPS
UNG
UPF2
UPF3B
UPP1
URB2
USP1
USP10
USP11
USP22
USP27X
USP31
USP33
USP40
USP46
USP49
USP6NL
UST
UTP14A
UTP18
UTP20
UTP6
VAC14
VANGL2
VAX2
VCL
VDR
VKORC1L1
VMN1R58
VMN2R96
VWA1
WDFY4
WDHD1
WDR3
WDR35
WDR36
WDR43
WDR47
WDR60
WDR61
WDR62
WDR75
WDR92
WDYHV1
WFDC16
WHRN
WNT2B
WRB
WWC2
XKRX
XPO5
XRCC1

XRCC2
XYLB
XYLT2
YARS2
YBX2
YDJC
YEATS2
YLPM1
ZADH2
ZBTB17
ZBTB46
ZC3H12A
ZC3H12C
ZC3H12D
ZC3H8
ZCCHC14
ZCRB1
ZDHHC13
ZDHHC14
ZDHHC6
ZFC3H1
ZFHX3
ZFP101
ZFP131
ZFP28
ZFP318
ZFP382
ZFP410
ZFP428
ZFP449
ZFP451
ZFP488
ZFP518B
ZFP52
ZFP609
ZFP667
ZFP85-RS1
ZFP870
ZFP9
ZFP90
ZFYVE26
ZFYVE9
ZGPAT
ZIK1
ZMAT3
ZMYM1
ZMYND19
ZNHIT6
ZSCAN21
ZSCAN22
ZWILCH
ZZZ3

Supplementary Table 2. List of shared upstream regulators and canonical pathways in each group. Numbers indicate –logP values of an enrichment score of each upstream regulator or canonical pathways. The list shows ones highly significant to all subsets in each group (–logP>3 or P<0.001 for upstream regulators and –logP>1.3 or P<0.05 for canonical pathways). For L2 and L3 groups, canonical pathways significantly shared by three out of four subsets are shown.

Group	Upstram Regulator	NKT1	ILC1	V5	Th1	NK
L1	ITK	30.10	12.31	10.66	13.83	11.15
	IL2	18.61	9.79	13.85	14.82	11.72
	IL12 (complex)	18.16	7.51	7.83	21.00	8.73
	IL21	14.90	12.67	12.60	8.84	10.31
	IL15	14.23	8.58	12.37	12.91	8.36
	IFNG	12.96	8.35	14.35	29.79	9.73
	TCR	11.53	5.25	9.68	17.82	6.68
	IL4	11.16	11.71	11.25	15.19	6.69
	IL10	10.34	4.90	6.25	10.44	6.69
	TGFB1	9.29	11.09	10.18	23.16	12.61
	TNF	9.24	6.64	12.47	20.31	7.01
	CSF2	8.74	5.16	5.73	7.30	4.99
	CD28	8.70	3.47	6.57	9.39	3.14
	FAS	8.17	5.23	5.95	10.38	4.15
	CD3	7.99	5.29	10.75	7.65	5.24
	IL5	7.79	6.92	7.85	15.14	8.45
	STAT3	7.50	3.77	7.73	20.16	3.65
	IL1B	7.40	4.07	4.69	9.28	4.57
	ESR1	7.33	5.60	8.50	12.79	3.74
	TLR4	7.24	4.35	9.20	9.16	3.46
	CREBBP	7.08	6.83	9.60	11.52	7.29
	ID2	7.04	4.45	8.90	11.03	5.80
	Interferon alpha	6.73	6.23	4.58	20.54	4.50
	IFN alpha/beta	6.30	3.04	3.68	6.68	3.39
	SATB1	6.13	8.71	5.78	4.84	6.76
	ID3	5.85	4.29	9.51	10.59	5.60
	ERBB2	5.78	6.80	3.42	15.57	5.67
	ETS1	5.32	5.05	6.08	5.45	5.51
	IgG	5.15	4.62	3.62	5.44	3.89
	IRF3	5.13	4.60	3.54	12.98	3.24
	IFNA2	5.10	5.46	3.80	24.48	3.36
	CD40LG	4.69	3.41	7.58	13.93	3.96
	IRF7	4.21	7.03	3.67	17.35	4.59
	CSF3	4.18	4.60	6.57	4.84	6.76
	FOXO1	3.69	4.00	3.61	5.85	3.63
	PI3K (complex)	3.53	6.96	5.15	3.45	7.79
	CD38	3.43	5.60	3.82	12.86	5.52
	CCL5	3.04	4.18	3.97	3.52	4.55
	EP300	3.04	9.57	3.64	8.79	6.66
		NKT2	ILC2	V6	Th2	
L2	TP53	12.31	6.72	23.02	7.46	
	CSF2	11.46	8.29	25.52	5.93	
	ID2	7.60	12.20	13.82	5.95	
	ID3	7.42	12.96	14.51	5.66	
	RRP1B	6.39	7.88	8.03	4.17	
	TGFB1	5.84	6.31	15.00	6.31	
	ESR1	5.77	5.35	6.73	3.83	
	CD3	5.15	9.98	11.15	4.43	
	ERBB2	4.51	6.17	13.15	3.77	
	TCR	3.72	6.73	12.59	5.88	
	MYC	3.27	3.85	10.69	3.13	
		NKT17	ILC3	V2	Th17	
L3	ID3	5.76	6.11	7.11	4.75	
	ID2	4.84	7.12	7.28	3.78	
	BCL6	3.35	3.51	4.16	4.90	
	EP300	3.19	6.25	16.43	5.53	
	IL4	3.06	4.92	6.00	7.43	

Group	Canonical Pathway	NKT1	ILC1	V5	Th1	NK
L1	Natural Killer Cell Signaling	10.86	8.52	6.27	5.43	9.39
	Pathogenesis of Multiple Sclerosis	4.65	2.10	3.44	2.34	1.95
	Crosstalk between Dendritic Cells and Natural Killer Cells	3.50	2.56	1.75	4.19	2.18
	Production of Nitric Oxide and Reactive Oxygen Species in Macrophages	2.84	1.58	4.12	4.16	1.64
	Integrin Signaling	2.60	7.54	6.31	6.47	9.46
	Germ Cell-Sertoli Cell Junction Signaling	2.35	2.99	4.00	3.96	1.95
	Type I Diabetes Mellitus Signaling	2.21	3.47	1.41	5.00	1.76
	PKCθ Signaling in T Lymphocytes	2.07	3.20	4.39	3.38	1.58
	Erythropoietin Signaling	1.96	1.63	2.95	3.31	1.39
	Leukocyte Extravasation Signaling	1.95	2.87	2.62	1.72	2.81
	CCR5 Signaling in Macrophages	1.89	4.72	5.40	3.12	2.60
	Chemokine Signaling	1.88	1.54	3.58	3.07	1.89
	TREM1 Signaling	1.86	3.76	3.55	3.64	3.28
	Reelin Signaling in Neurons	1.82	3.65	3.44	2.89	2.46
	Ceramide Signaling	1.75	2.71	4.94	2.17	3.02
	Cytotoxic T Lymphocyte-mediated Apoptosis of Target Cells	1.73	5.07	3.75	3.62	2.56
	Virus Entry via Endocytic Pathways	1.61	4.78	2.28	4.56	5.82
	NF-κB Signaling	1.57	1.75	2.60	1.64	1.38
	Paxillin Signaling	1.54	5.42	5.11	4.26	5.56
	Pancreatic Adenocarcinoma Signaling	1.47	2.17	1.45	1.51	1.30
	Role of Pattern Recognition Receptors in Recognition of Bacteria and Viruses	1.31	2.47	2.29	3.79	1.54
	p70S6K Signaling	1.31	1.88	5.07	3.79	2.63
		NKT2	ILC2	V6	Th2	
L2	cAMP-mediated signaling	2.24	3.46	0.00	1.86	
	Protein Kinase A Signaling	2.07	2.09	0.66	3.35	
	G-Protein Coupled Receptor Signaling	1.90	3.48	0.00	1.53	
	T Helper Cell Differentiation	1.81	3.68	2.42	0.51	
	Altered T Cell and B Cell Signaling in Rheumatoid Arthritis	1.58	3.20	2.77	0.35	
	Airway Inflammation in Asthma	1.45	4.79	2.70	0.75	
		NKT17	ILC3	V2	Th17	
L3	Inhibition of Matrix Metalloproteases	1.77	1.53	3.57	1.18	
	Type I Diabetes Mellitus Signaling	1.75	1.95	1.25	1.85	